UNIVERSITY OF CALIFORNIA

Los Angeles

Analysis of a Feed Bypass Modification to a Reverse Osmosis System

A thesis submitted in partial satisfaction

of the requirements for the degree Master of Science

in Civil Engineering

by

Richard Newell Franks II

2000

The thesis of Richard Newell Franks II is approved.

Keith D. Stolzenbach

Ivan Catton

Michael K. Stenstrom, Committee Chair

University of California, Los Angeles

2000

Table of Contents

1.0 Introduction 1

2.0 Review 3

2.1 Reverse Osmosis Defined 3

2.2 Reverse Osmosis Process 5

2.3 Reverse Osmosis Theory 7

2.4 Membrane Performance 8

2.5 Spiral Wound Membrane 9

2.5.1 Design 9

2.5.2 Modifications 12

2.5.3 Adverse Effects 13

3.0 Feed Flow Bypass 16

3.1 System Modification 16

3.2 Effects of Feed Bypass on System Performance 18

3.2.1 Variation on Inlet Flow Rates 18

3.2.2 Variation on Inlet Concentrations 19

4.0 Model Development 21

4.1 Forward Averaging Model Geometry 21

4.2 Cell Mass Transport Models 23

4.2.1 Solvent Mass Transport 23

4.2.2 Solute Mass Transport 24

4.2.3 Solution Mass Transport 25

4.3 Cell Permeate Conditions 27

4.4 Cell Exit Conditions 28

4.5 Whole Membrane Solutions 28

4.6 Modifications to Forward Averaging Model 34

4.6.1 Spreadsheet 34

4.6.2 System Feed Flow Bypass 34

4.6.3 Brackish Solutions 37

5.0 Results and Discussion 43

5.1 Model Test 43

5.2 Feed Bypass Modeled 51

5.3 Detailed Analysis 57

5.3.1 Analysis of Bypass Flow Rate 57

5.4.2 Bypass Ratios 65

5.5 System Comparison 71

5.5.1 Flow Variations 71

5.5.2 Membrane Variations 78

5.6 System Advantages 81

6.0 Conclusions 82

8.0 Appendix 84

9.0 References 85

List of Figures

List of Tables

List of Symbols

Ac	high pressure channel cross-sectional area
C	concentration (kg/m^3)
Dab	Diffusivity of Solution (m^2/s)
Dam K/τ	solute mass transport parameter through membrane (m/s)
H	cell height = high pressure channel height (m)
J	volumetric flux ($m^3/m^2/s$)
k	mass transfer coefficient (m/s)
K_B	solvent permeability coefficient (m/s/kPa)
KM	mesh step mixing coefficient ($m^{-1/2}$)
$K\pi$	osmotic pressure constant ($kPa/kg/m^3$)
L	spiral wound membrane length (m)
N	number of cells per membrane
P	pressure (kPa)
Q	flow rate (m^3/s)
S	cell surface area (m^2)
W	cell width (m)
X	cell length (m)

Greek Symbols

Δ	change across membrane
π	osmotic pressure (kPa)
ρ	solution density (kg/m^3)
ν	solution kinematic viscosity (m^2/s)

Subscripts

B	solvent
e	exit/reject
mem	whole membrane
n	nth cell
o	inlet of feed
p	permeate
s	solute
sys	reverse osmosis system consisting of one or more spiral wound membranes within a single pressure vessel
w	membrane wall

Acknowledgments

ABSTRACT OF THE THESIS

Analysis of a Feed Bypass Modification

to a Reverse Osmosis System

by

Richard Newell Franks II

Master of Science in Civil Engineering

University of California, Los Angeles, 2000

Professor Michael K. Stenstrom, Chair

An analysis was conducted on a proposed reverse osmosis pressure vessel modification which would allow a portion of the inlet feed flow to bypass the first membrane and enter subsequent membranes within the same pressure vessel. The analysis was conducted through the modification of an existing theoretical model using a spreadsheet program. Whole system response, as well as individual membrane response, to variations in the quantity of flow diverted past the first membrane was analyzed. The analysis indicated an increase in recovery would occur in conjunction with a decrease in separation as flow was diverted past the first membrane and allowed to enter subsequent membranes.

1.0 Introduction

As world population climbs above six billion, greater stress is placed on the earths natural resources, especially its limited supply of fresh water. Though climate and technology influence access to water, the single greatest factor influencing the availability of existing fresh water is the number of people competing for it (Gardner and Engleman, 1997). The already limited supply of fresh water is itself being diminished by the contamination that accompanies large scale industrialization, especially in third world countries.

The environmental threat to a limited water supply, along with a growing demand for water, necessitates the advancement of water treatment technology. In particular, there is a need to advance treatment of water by reverse osmosis beyond its present applications and overcome limitations associated with membrane technology such as fouling, pressure losses and concentrations polarization. This will most likely be done, as one author points out, through slow and incremental advances (Simon, 1998).

A proposed advance would modify the traditional reverse osmosis system, with spiral wound membranes in series, to allow a portion of the feed flow to bypass the first membrane within a pressure vessel and enter subsequent membranes within that same pressure vessel (Chancellor et al., 1998).

The goal of this study is to compare the performance of a traditional reverse osmosis system with the proposed feed bypass system. The analysis will be performed theoretically by modifying a model available in the literature to simulate the feed bypass. The model will be used to determine the system's response to feed bypass as well as compare the performance of a feed bypass system with that of a traditional system.

2.0 Review

2.1 Reverse Osmosis Defined

Reverse osmosis (RO) is a solution separation process in which a solvent (usually water) is passed through a semi permeable membrane while both suspended solids and solute are retained. The solvent is passed through the membrane by applying a pressure that overcomes the solutions natural osmotic pressure (Figure 2.1). In the absence of applied pressure, the pure solvent flow through a semi permeable membrane will be from the side of lesser concentration to that of greater concentration (Figure2.2) until osmotic equilibrium is achieved and the pressure difference between the two sides of the membrane is equal to the osmotic pressure (Figure 2.3)(Byrne, 1995; Bhattacharyya and Williams, 1992)

Though the first recorded observation of the osmotic process occurred over 200 years ago, modern RO research began relatively recently in the 1950s at both the University of California, Los Angeles and the University of Florida (Glater, 1998). Since that time, the RO process has been applied in such areas as water/wastewater treatment, desalination, and mineral recovery. A range of industries such as food and beverage, pulp and paper, and medical and pharmaceutical, also utilize reverse osmosis.

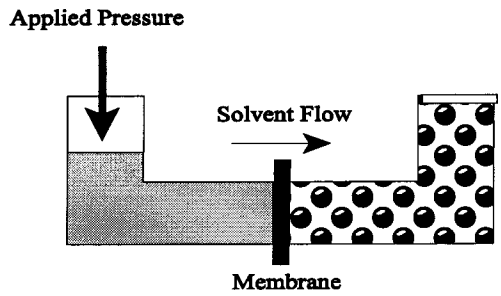

Figure 2.1 Reverse osmosis process in which the applied pressure forces the solvent through the membrane and leaves behind a more concentrated solution.

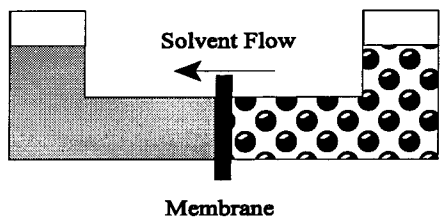

Figure 2.2 Natural osmosis in which the solvent flows from the side of lesser concentration to that of greater concentration.

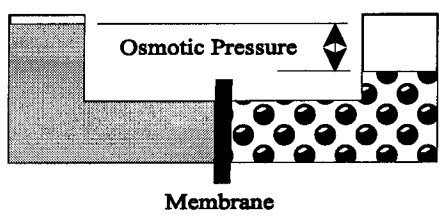

Figure 2.3 Osmotic equilibrium in which the pressure difference between the two sides of the membrane is equal to the osmotic pressure.

2.2 Reverse Osmosis Process

Reverse osmosis, illustrated in Figure 2.4, occurs when a feed solution, with a given concentration (Co), flows over the membrane surface at a flow rate (Qo). If the feed solution pressure (Po) is greater than the solution's osmotic pressure, then solvent flux (J_B) will occur through the membrane in a direction opposite to that of natural osmosis. Though much less than the solvent flux, a solute flux (Js) occurs which is dependent on the concentration differential across the membrane surface.

Because only a fraction of the feed flow passes through the membrane, the system produces two separate effluent flows. The flow which passes through the membrane (Qp) is termed the permeate and possess a much lower concentration (Cp) than both the original feed flow and the concentrate flow (Qe), or reject, that remains. As the water passes through the membrane, it leaves behind a solution with higher concentration at the membrane wall (Cw). Due to pressure losses in the membrane channel, the concentrate flow leaving the element will be at a slightly lower pressure (Pe) than the feed pressure.

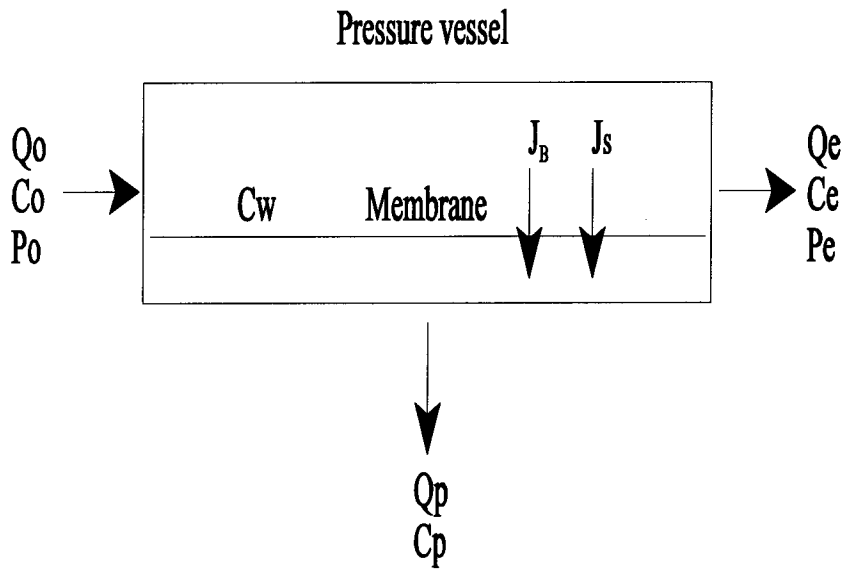

Figure 2.4 The reverse osmosis process for a single membrane.

2.3 Reverse Osmosis Theory

Though several different specific models have been developed to describe passage through a membrane (Bhattacharyya, 1992), a general theory is described below.

The passage of solvent through the membrane can be described by:

$$J_B = \frac{Q_p}{S} = K_B (\Delta P - \Delta \pi) \tag{2.1}$$

Where

Q_p = permeate flow rate

S = membrane surface area

K_B = solvent permeability coefficient

ΔP = differential pressure across the membrane surface

$\Delta \pi$ = differential osmotic pressure across the membrane surface

The passage of solute through the membrane can be described by:

$$J_s = \frac{K_s}{\tau} \Delta C \tag{2.2}$$

Where:

K_s = membrane permeability coefficient for the solute

τ = membrane thickness

ΔC = differential solute concentration across the membrane

2.4 Membrane Performance

The performance of an RO membrane is usually determined by three parameters: solvent flux through the membrane, recovery and separation (Winston, 1992). The solvent flux is given in Equation (2.1). The recovery of a system is its ratio of permeate flow rate (Qp) to feed flow rate (Qo), given by:

$$Y = Qp / Qo \tag{2.3}$$

The separation of a system is an indication of the membrane's ability to reject salts while allowing for the passage of solvents. Separation is given by:

$$f = 1 - Co/Cp \tag{2.4}$$

Where

Co = initial feed concentration

Cp = permeate concentration

2.5 Spiral Wound Membrane

2.5.1 Design

With the emergence of RO technology came four designs to maximize the efficiency and performance of the membranes. These four designs include: plate-and-frame, tubular, hollow fiber, and spiral wound membranes. Though modifications have been made to these four original designs, no new designs have been devised since their development in the 1960s (Matsuura, 1993).

The spiral wound membrane (SWM) has emerged as one of the more widely used designs, partly due to its ability to contain a large membrane area in a relatively small volume. It is assembled by rolling a rectangular sandwich of two or more membranes, separated by a permeate carrier, around a central permeate collection tube. The SWM is then inserted into a pressure vessel to form what will be refered to in this paper as the spiral wound membrane system or SWM system.

The original designs for a single SWM in a pressure tight container originated with Merton and Bray of Gulf General Atomic Inc. in 1968 (pat 3,386,583 and pat.

3,417,870). Nearly ten years later, Bray submitted pat 4,046,685 describing several membranes stacked in series within a single pressure vessel (Scott, 1981). In this system, a peripheral seal forces the total feed flow to pass longitudinally through each membrane in series so that the reject from the first membrane becomes the feed for the next membrane. This configuration allows for more than one membrane to take advantage of the pressure applied to a single pressure vessel (Figure 2.5).

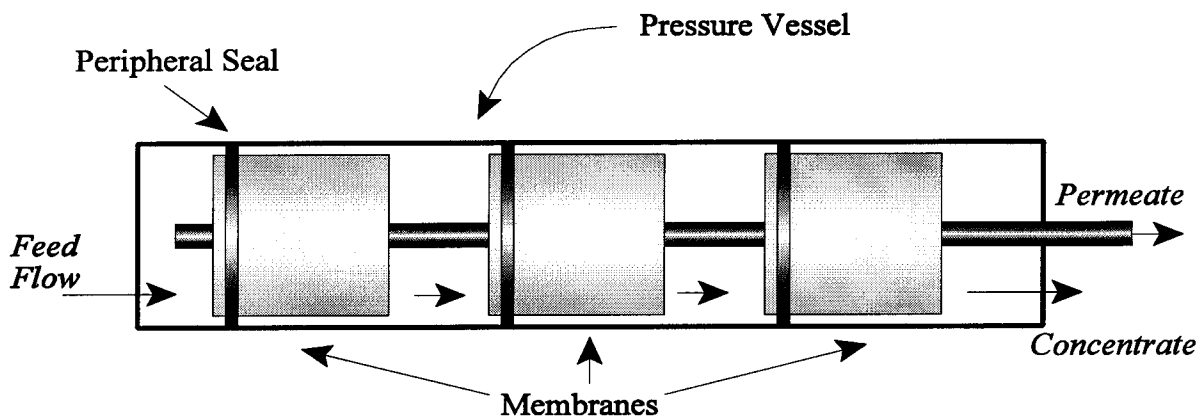

Figure 2.5 A traditional spiral wound membrane system. A single pressure vessel contains one or more spiral wound membranes in series. The peripheral seal prevents flow from bypassing any of the membranes.

2.5.2 Modifications

The placement of SWMs in series in a single pressure vessel has become the industry standard with only minor modifications to the pressure vessel flow configuration since the original Bray design in 1977. One such modification places small slots in the peripheral seals as well as flow channels on the outer membrane surface. The sole purpose of the modification is to flush the otherwise dead space between the outer surface of the membrane and the wall of the pressure vessel (Matsuura, 1993).

Another substantial modification was developed in the Netherlands (Wessels, 1998). Though intended for low pressure nano- and ultra-filtration, the design is a modification of the same fundamental SWM system used for reverse osmosis. In this modification, feed flow is allowed to enter from both ends of the pressure vessel which is designed with a slightly larger diameter than membranes so as to allow a portion of the flow to bypass the first membrane and enter subsequent membranes. The design modification was shown to have several advantages:

- A slight increase in permeate flux through the elements occurred when compared to the traditional design.
- The larger diameter pressure vessels eliminated the dead space between the membranes and pressure vessel wall thus reducing the contamination of the membranes.

- The membranes were also much easier to insert and remove due to the larger diameter of the pressure vessel.

2.5.3 Adverse Effects

Despite modifications to SWM system, limitations still exist that prevent the RO process from becoming a more widely accepted form of water purification, especially for large scale municipal applications. Several obstacles, including hydraulic pressure losses, concentration polarization, and fouling, hinder the improved performance of the SWM system.

Concentration Polarization

Concentration polarization can be defined as an increase in solute concentration at the membrane wall (relative to the bulk concentration) caused by the convective flow of solute to the wall being greater than the solute's rate of diffusion away from the wall. The negative effects of concentration polarization include:

- A decrease in permeate flow.
- An increase in solute passage through the membrane.
- A contributor to fouling (Bhattacharyya and Williams, 1992).

Fouling

Fouling is an accumulation of particulate mater on the membrane surface which results in the plugging of the membrane and therefore a decrease in the permeate flow (Bhattacharyya and Williams, 1992). Foulants can be classified in three broad categories:

1. sparingly soluble inorganic compounds,
2. particulate matter, and
3. dissolved organic compounds (Potts et al. 1981).

To reduce concentration polarization and fouling, SWMs are designed with a plastic netting inserted between the membrane leafs to increase flow turbulence and thus increase mixing. The drawback to the increased turbulence is an increase in hydraulic pressure losses through the length of the membrane.

Hydraulic Pressure Losses

A slight drop in hydraulic pressure occurs as the flow moves through the concentrate channel of a SWM. This pressure drop, which increases with increasing flow rate, is caused by viscous drag on the spacers and channel walls, fluid forces on the spacers, and changes in flow direction (Da Costa et al, 1994). The loss of pressure has an adverse effect on the membrane performance by reducing solvent flux as is evident from the previously stated solvent transport equation (Equation 2.1).

The negative effects produced by a single membrane are compounded as flow passes through each subsequent membrane in a single pressure vessel. Despite the decrease in productivity, membranes are placed in series in order to take full advantage of the available driving pressure (Carnahan, 1999).

3.0 Feed Flow Bypass

3.1 System Modification

A suggested modification to the traditional SWM system alters flow patterns within the pressure vessel (Chancellor et al., 1998). The modification diverts a percentage of feed flow past the first membrane and into subsequent membranes within the same pressure vessel (Figure 3.1). A portion of the diverted flow mixes with the concentrate of the first membrane and serve as influent to the subsequent membrane. This process is repeated so that the influent to each membrane (except the first) housed within a single pressure vessel is a mixture of concentrate from the previous membrane as well as a portion of the original feed flow.

When compared to the traditional SWM system, the modification, referred to as the feed bypass system, alters the flow rates and concentrations seen by each membrane. This alteration of flow rates and concentrations should impact the overall performance of the system.

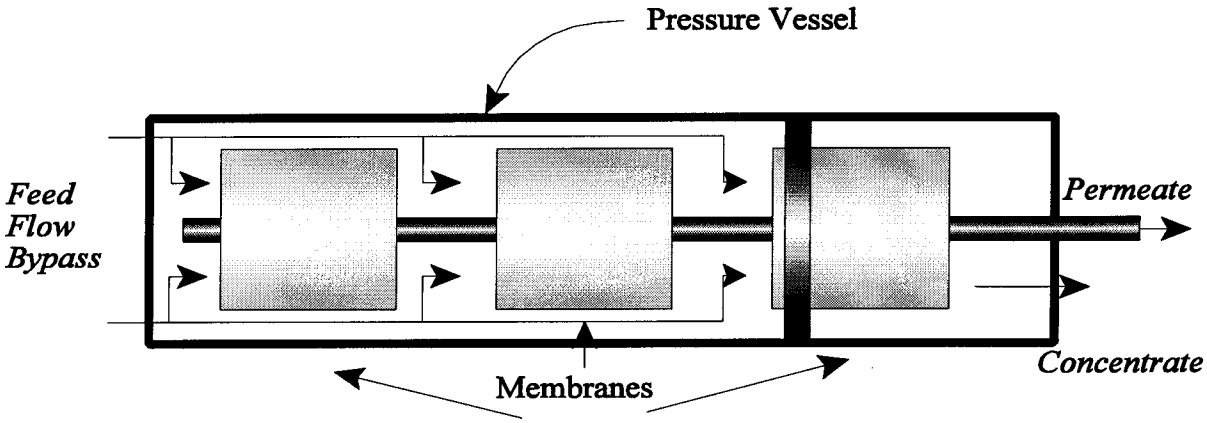

Figure 3.1 A feed bypass system. The absence of a peripheral seal on membranes 1 and 2 allows for a percentage of the feed flow to bypass the first membrane and enter membranes 2 and 3.

3.2 Effects of Feed Bypass on System Performance

The performance of a traditional SWM system is, to a certain extent, an optimization problem (Polyakov 1996). In the same way, the performance of a feed bypass system is an optimization problem in as much as the diversion of a percentage of the flow around the first membrane effects the inlet flow and inlet concentration of all membranes within the module. The variation in flow and concentration seen by each membrane will have both a positive and negative effect on the overall performance of those membranes.

3.2.1 Variation on Inlet Flow Rates

Flow through a spiral wound membrane has a significant effect on permeate flux and separation performance. Both permeate flux and separation are indirectly influenced by the turbulence that accompanies increased flow rate. As mentioned in chapter 2, the turbulence serves to mix the highly concentrated wall solution with the less concentrated bulk solution which reduces the effects of concentration polarization and fouling, thus increasing salt rejection and permeate flux. This same turbulence has the negative effect of increasing the hydraulic pressure loss along the length of a membrane channel. As noted in Chapter 2, the drop in pressure leads to a decrease in permeate flux.

The increase in flow through the downstream membranes of a feed bypass system

will therefore cause an increase in separation performance of those elements while effecting permeate flux both positively and negatively. Inversely, the decrease in flow through the first element will decrease separation while effecting permeate flux both positively and negatively.

3.2.2 Variation on Inlet Concentrations

Like flow rate, the solute concentration entering a membrane element effects both the permeate flux and separation performance of that element. Specifically, an increase in concentration increases the solutions osmotic pressure which, according to Equation 2.1, decreases solvent flux.

The concentration of the flow entering a membrane element affects the performance of the membrane by affecting the magnitude of concentration polarization. The greater the concentration in the flow, the greater the concentration at the membrane boundary which results in a greater solute flux. In contrast, a decrease in inlet concentration has been modeled to show an increase in concentration polarization (Madireddi et al, 1999). This increase in concentration polarization, caused by the increase in permeate flux which comes with a lower concentration, finally hinders separation performance.

Variation in concentration will also effect some forms of fouling. An increase in

concentration polarization to the point of solute saturation leads to the precipitation of certain inorganic molecules which form a gel on the membrane surface (Potts, 1981).

The changes in flow rates and concentrations associated with a feed bypass system should impact the performance of the system. The overall performance of a feed bypass system is analyzed theoretically in Chapter 5 using a forward averaging model.

4.0 Model Development

4.1 Forward Averaging Model Geometry

A theoretical comparison was made between the traditional flow configuration through a pressure vessel containing spiral wound membranes and the feed bypass configuration. The comparison was based on modifications made to a forward averaging model for dilute solutions developed by Dickson et al. (1992). The forward averaging model divides a hypothetical unwound membrane into discrete cells (Figure 4.1).

Assuming plug flow conditions through any given cell n, the inlet conditions (flow rate, concentration, and pressure) to cell n are applied to a set of mass transfer, mass flow, and empirical equations to calculate the permeate and exit conditions from cell n. The exit conditions are then used as the inlet conditions for cell n+1 (Figure 4.2). The inlet conditions for the first cell (n=1) are equivalent to the feed conditions of the overall membrane while the exit conditions from the last cell (n=final) are equivalent to the reject conditions of the overall membrane.

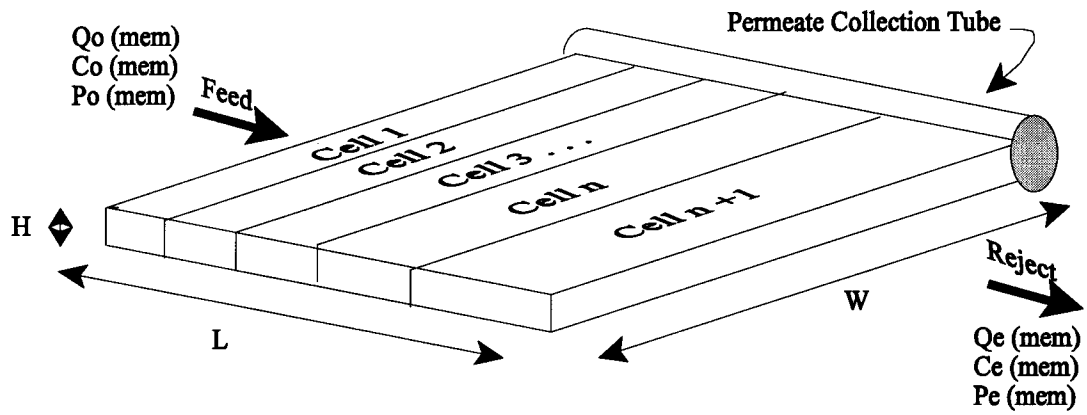

Figure 4.1 Unwound membrane divided into discrete cells for the forward averaging model.

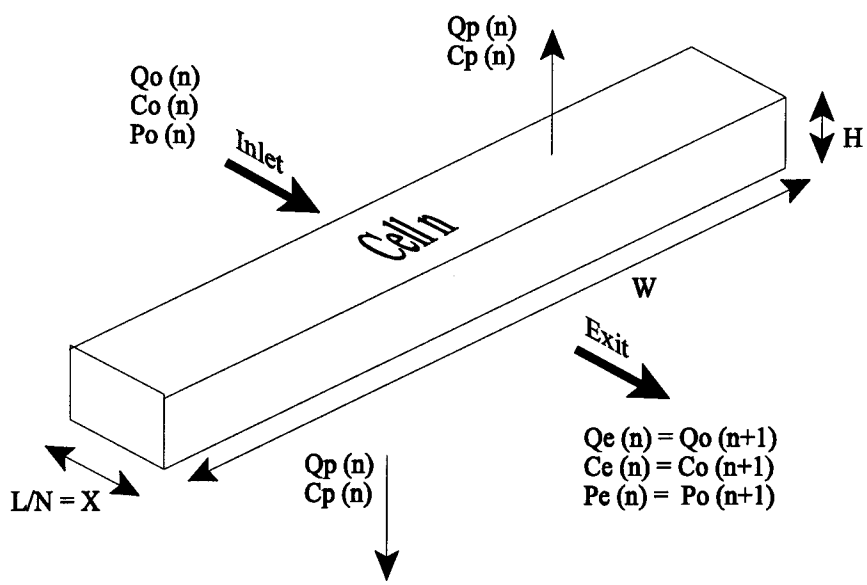

Figure 4.2 A single cell n of the forward averaging model.

4.2 Cell Mass Transport Models

Three mass transport models, along with dilute solution assumptions, allow the permeate conditions leaving cell n to be easily calculated. The three mass transport models are derived from a generalized capillary flow model developed by Kimura and Sourirajan known as the Kimura-Souririjan Analysis or KSA (Sourirajan, 1970). Each of the three models and their corresponding simplified equations are discussed below.

4.2.1 Solvent Mass Transport

The first mass transport model gives the following permeate flux for the solvent:

$$J_B = K_B (\Delta P - \Delta \pi) \tag{4.1}$$

The solvent permeability constant K_B, determined experimentally, is specific to both the membrane and solution.

Two simplifications can be made to Equation (4.1). First, if the permeate pressure is atmospheric, then the transmembrane pressure, ΔP, is equivalent to the inlet pressure, Po. Second, if the solution is dilute, then the osmotic pressure differential is much less than the transmembrane pressure and Equation (4.1) can therefore be simplified to:

$$J_B = K_B (P_o) \tag{4.2}$$

4.2.2 Solute Mass Transport

The second mass transport model derived from the KSA gives the following permeate flux for the solute:

$$J_s = \frac{D_{am} K}{\tau \rho} (C_w - C_p) \tag{4.3}$$

The solute transport parameter $\left(\frac{D_{am} K}{\tau}\right)$ in Equation (4.3) is a combination of three separate parameters: solute diffusivity through the membrane (D_{am}), a factor relating solute concentration in the membrane to solute concentration in the solution (K), and the film thickness (τ). Though it would be difficult to accurately measure each of the three parameters separately, the combined solute transport parameter can be determined experimentally.

According to the KSA, Equation (4.3) can be rewritten in terms of solvent flux if it is first considered that

$$\frac{J_s}{(J_s + J_B)} = \frac{C_p}{\rho} \tag{4.4}$$

and, for dilute solutions,

$$J_s + J_B \approx J_B \tag{4.5}$$

Equation (4.4) then becomes

$$J_s = \frac{J_B C_p}{\rho} \tag{4.6}$$

and Equation (4.3) can be rewritten as

$$J_B = \frac{D_{am} K}{\tau} \left(\frac{C_w - C_p}{C_p} \right) \tag{4.7}$$

4.2.3 Solution Mass Transport

The third mass transport model in the KSA accounts for the concentration polarization phenomenon and relates the bulk, wall, and permeate concentrations to the permeate flux of the solution:

$$J_B + J_s = k \ \ln\left(\frac{C_w - C_p}{C_o - C_p}\right) \tag{4.8}$$

The mass transfer coefficient k in Equation (4.8) is a function of solute diffusivity, solution viscosity, flow channel geometry, and feed flow rate. The equation developed by Dickson for k is based on a mesh step model developed by Winograd et al. (1973) and results in:

$$k = \frac{KM \ D^{2/3} Q_o^{1/2}}{\nu^{1/6} A_c^{1/2}} \tag{4.9}$$

In Equation (4.9), the mesh step mixing coefficient KM is composed of two constants, the mesh step pitch, M, and the mixing efficiency, Ke, both of which are functions of spacer geometry within the high pressure flow channel of the spiral wound membrane.

When a dilute solution is considered then

$$J_s + J_B \approx J_B \tag{4.10}$$

and Equation (4.8) becomes

$$J_B = k \ln\left(\frac{C_w - C_p}{C_o - C_p}\right) \tag{4.11}$$

4.3 Cell Permeate Conditions

The three equations derived from the KSA mass transport models, can be rearranged and solved simultaneously to determine the permeate conditions for cell n. Equation (4.2), when multiplied by the surface area of the cell, yields the permeate flow rate.

$$Q_p = J_B S \tag{4.12}$$

Equation (4.7) can be rearranged to give

$$\frac{C_p}{C_w} = \frac{D_{am} K/\tau}{J_w + D_{am} K/\tau} \tag{4.13}$$

The solution to Equations (4.13) and (4.2) can be used in a rearranged form of Equation (4.11) to give

$$\frac{C_o}{C_w} = \frac{C_p}{C_w} + \left[1 - \left(\frac{C_p}{C_w}\right) e^{-(J_B/k)}\right] \tag{4.14}$$

Equations (4.13) and Equation (4.14) can be solved simultaneously to determine the membrane wall concentration, C_w, and the permeate concentration, C_p, of cell n.

4.4 Cell Exit Conditions

With the newly acquired permeate conditions from cell n, the exit conditions may now be computed using mass balance equations:

$$Q_e = Q_o - Q_p \tag{4.15}$$

and

$$C_e = \frac{C_o Q_o - C_p Q_p}{Q_e} \tag{4.16}$$

The exit pressure from cell n is given by an empirical equation available in the literature (FilmTec, 1984 as cited by Dickson, 1992):

$$P_e = P_o - \left[165 \times 10^6 \, (Q_o) \, X\right] \tag{4.17}$$

4.5 Whole Membrane Solutions

As stated before, the final reject conditions from the whole membrane are equal to the exit conditions from the last cell. The final permeate conditions, on the other hand, require some simple calculations. The final permeate flow rate from the whole

membrane is the sum of the permeate flow rates from each cell n.

$$Q_{p(mem)} = \sum_{n=1}^{n} Q_{p(n)} \tag{4.18}$$

The final permeate concentration is derived from the permeate flow rates and concentrations from each cell n.

$$C_{p(mem)} = \frac{\sum_{n=1}^{n} Q_{p(n)} C_{p(n)}}{Q_{p(mem)}} \tag{4.19}$$

Finally, the overall recovery ,Y(mem), and separation, f(mem), of the membrane can be calculated as:

$$Y_{(mem)} = \frac{Q_{e(mem)}}{Q_{o(mem)}} \tag{4.20}$$

$$f_{(mem)} = \frac{C_{o(mem)} - C_{p(mem)}}{C_{o(mem)}} \tag{4.21}$$

A summary of the formulas used to calculate the conditions in cell n of the

forward averaging model can be found in Table 4.1 while the necessary model inputs can be found in Table 4.2. A flow diagram of the computational procedure is shown in Figure 4.3.

Equation No.	Formula
4.9	$k = \dfrac{KM\ D^{2/3}\ Q_o^{1/2}}{\nu^{1/6} A_c^{1/2}}$
4.2	$J_B = K_B\ (P_o)$
4.13	$\dfrac{C_p}{C_w} = \dfrac{D_{am}\ K/\tau}{J_w + D_{am}\ K/\tau}$
4.14	$\dfrac{C_o}{C_w} = \dfrac{C_p}{C_w} + \left[1 - \left(\dfrac{C_p}{C_w}\right) e^{-(J_B/k)}\right]$
4.12	$Q_p = J_w\ S$
4.17	$P_e = P_o - \left[165 \times 10^6\ (Q_o)\ X\right]$
4.15	$Q_e = Q_o - Q_p$
4.16	$C_e = \dfrac{C_o\ Q_o - C_p\ Q_p}{Q_e}$

Table 4.1 Equations for calculating conditions in cell n. Exit conditions from cell n are used as inlet conditions for cell n+1. Equations are presented in the same order that they are calculated within the forward average algorithm (Figure 4.3).

Symbols	Units	Definitions
Solution constants		
K_B	m/ s / kPa	solvent permeability coefficient
ν	m^2/s	solution kinematic viscosity
D	m^2/s	diffusivity
Membrane constants		
Ac	m^2	high pressure channel cross sectional area
KM	$m^{-1/2}$	mesh step mixing coefficient
$D_{am}K/t$	m/s	mass transport parameter across membrane
S	m^2	cell area
X	m	cell length
W	m	channel width
H	m	channel height
N		number of cells per membrane element
L	m	element length
Flow Conditions		
$Q_{o(mem)}$	m^3/s	inlet feed flow
$C_{o(mem)}$	kg/m^3	inlet feed concentration
$P_{o(mem)}$	kPa	inlet feed pressure

Table 4.2 Inputs required for the forward averaging model

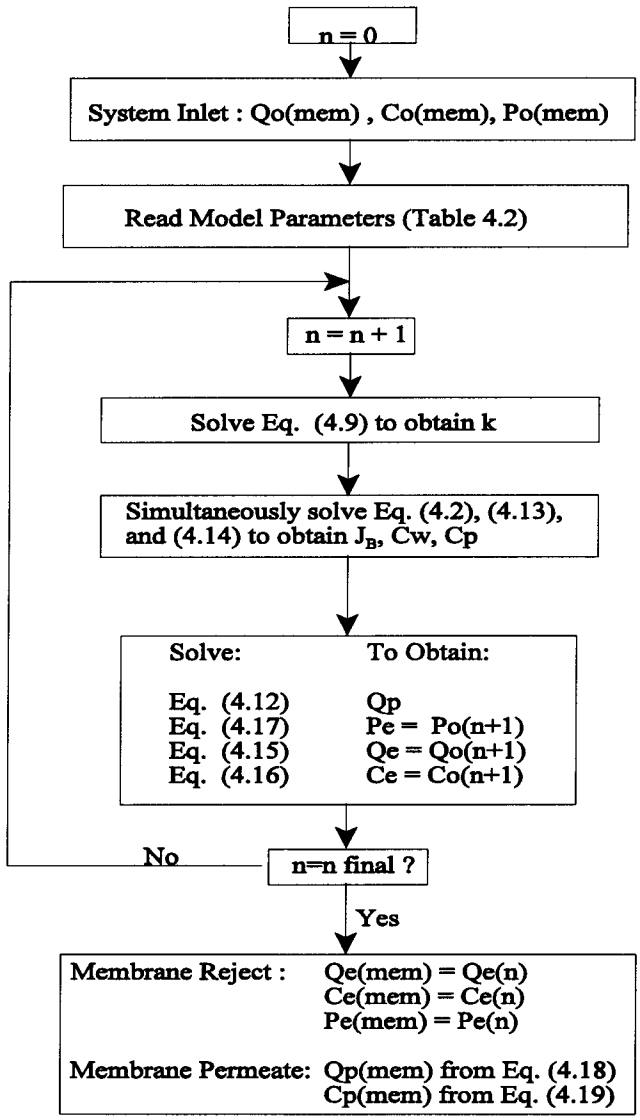

Figure 4.3 Computational procedure for the forward averaging model developed by Dickson et al.(1992).

4.6 Modifications to Forward Averaging Model

4.6.1 Spreadsheet

Though the forward averaging model was designed for a traditional computer program, it was easily constructed on a spreadsheet where the computations in Table 4.1 were performed in a single row on the spreadsheet. Each row on the spreadsheet corresponded to a cell in the membrane model until the number of rows equaled the desired number of cells to simulate a single membrane.

The first single membrane (membrane 1) was then copied twice within the same spreadsheet to create membrane 2 and 3. The reject conditions from membrane 1 (flow rate, concentration, and pressure) were used as the feed conditions for membrane 2 and the reject conditions from membrane 2 were used as the feed conditions for membrane 3. The result was the simulation of a reverse osmosis system consisting of three spiral wound membranes in series within a single pressure vessel (Figure 4.4).

4.6.2 System Feed Flow Bypass

To model the flow bypass of membrane 1, the spreadsheet was modified so that a percentage of the feed flow entering the system could be directed to membranes 2 and 3 as seen in Figure 4.5.

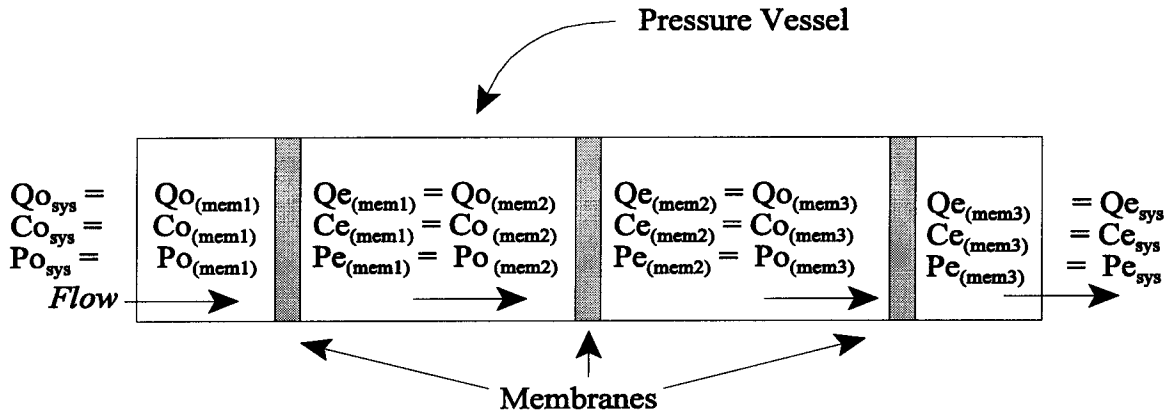

Figure 4.4 A traditional reverse osmosis pressure vessel containing three spiral wound membranes in series. Permeate flow not shown.

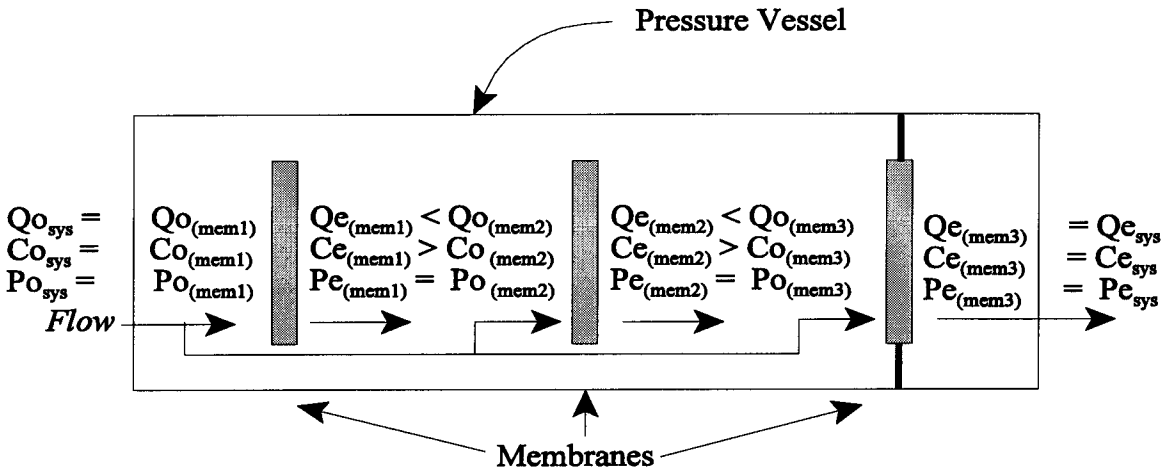

Figure 4.5 The effects of system feed flow bypass on the flow and concentration entering membranes 1, 2, and 3 in a single pressure vessel. Permeate flow not shown.

The designated percentage of system feed flow entering membrane 2 was added to the reject flow of membrane 1 to give the total feed flow entering membrane 2. For example, if 10% of the overall system feed flow were designated to enter membrane 2, then the total feed flow entering membrane 2 would be

$$Q_{o(mem2)} = 0.01Q_{o(sys)} + Q_{e(mem1)} \tag{4.21}$$

A similar calculation was performed to determine the total feed flow entering membrane 3.

The adjusted concentrations entering membranes 2 and 3 were derived from mass flow equations. Using the previous example where 10% of the system feed flow is designated for membrane 2, the concentration entering membrane 2 would be

$$C_{o(mem2)} = \frac{0.01Q_{o(sys)}C_{o(sys)} + Q_{e(mem1)}C_{e(mem1)}}{0.01Q_{o(sys)} + Q_{e(mem1)}} \tag{4.22}$$

The effects of system feed flow bypass on the feed pressures of membrane 1 and 2 were considered negligible. For this reason, the feed pressure of each membrane remained equal to the reject pressure of the previous membrane.

4.6.3 Brackish Solutions

The modified forward averaging model was designed to analyze the performance of a system treating dilute solutions. For the purposes of this study, it was desirable to analyze the performance of a system treating brackish solutions where concentrations would be greater and the effects of osmotic pressure on solvent flux could no longer be neglected. For analysis of brackish solutions, the osmotic pressure term was included in the solvent flux equation,

$$J_B = K_B (P_o - \pi) \tag{4.23}$$

and the osmotic pressure was computed by multiplying an osmotic pressure constant by the inlet concentration for any given cell,

$$\pi = K_\pi C_o \tag{4.24}$$

It is important to note that the actual method for computing the osmotic pressure of sodium chloride solutions involves multiplying an osmotic pressure constant K_π of approximately 79.3 kPa/kg/m3 (Byrne, 1995) by the wall concentration, not the inlet concentration. This could not be done in the forward averaging model because the solvent flux in each cell is computed before the wall concentration is known.

To reduce the error that would arise from using the inlet concentration instead of

the wall concentration to compute the solution's osmotic pressure, an amplified osmotic pressure constant of 275 kPa/kg/m3, was used. The amplified osmotic pressure constant was derived by trial and error using the outputs from a single membrane in the forward averaging model and comparing them to data from an actual ROGA-4000 membrane available in the literature (Ohya and Taniguchi, 1975). The comparison data used to obtain an amplified osmotic pressure constant of $K_{\pi} =$ 275 kPa/kg/m3 can be found in Table 4.3

Parameter	ROGA-4000	Model
Flow Rates (m3/s)		
Inlet	1.94×10^{-4}	1.94×10^{-4}
Permeate	2.50×10^{-5}	2.46×10^{-5}
Exit Flow	1.68×10^{-4}	1.69×10^{-4}
Concentrations (kg/m3)		
Inlet	2.6	2.6
Permeate	0.260	0.297
Exit	2.78	2.93
Pressures (kPa)		
Inlet	3447.38	3447.38
Exit	3343.96	3396.75

Table 4.3. Comparison of the inputs and outputs from the forward averaging model with published ROGA-4000 spiral wound membrane data (Ohya and Taniguchi, 1975). The data was used to obtain an amplified osmotic pressure constant of $K_\pi = 275$ kPa/kg/m3.

.

To test the range of applicability of the derived amplified osmotic pressure constant, the feed conditions of the forward averaging model were changed to match the feed conditions of different trials run on the ROGA-4000. The resulting model outputs, when compared to outputs of the ROGA-4000 (Table 4.4 and 4.5), show that the forward averaging model with an amplified osmotic pressure constant of 275 kPa/kg/m3 can adequately simulate the reverse osmosis process for brackish solutions with flow rates in the range of 0.0001 - 0.0003 m3/s and concentrations in the range of 2 - 3 kg/m3. Under these operating conditions, the model's accuracy was considered sufficient for the purpose of analyzing the effects of a feed bypass system treating brackish solutions. The results of the analysis of the feed bypass system treating brackish solutions are discussed in Chapter 5.

Parameter	ROGA-4000	Model
Flow Rates (m3/s)		
Inlet	3.01×10^{-4}	3.01×10^{-4}
Permeate	2.20×10^{-5}	1.91×10^{-5}
Exit Flow	2.79×10^{-4}	2.82×10^{-4}
Concentrations (kg/m3)		
Inlet	2.6	2.6
Permeate	0.260	0.245
Exit	2.71	2.76
Pressures (kPa)		
Inlet	2861.32	2861.32
Exit	2654.48	2748.45

Table 4.4. Comparison of the forward average model with data from the ROGA-4000 spiral wound membrane available in the literature (Ohya and Taniguchi, 1975) to test the range of applicability of the amplified osmotic pressure constant of $K_\pi = 275$ kPa/kg/m3.

Parameter	ROGA-4000	Model
Flow Rates (m3/s)		
Inlet	1.90×10^{-4}	1.90×10^{-4}
Permeate	2.80×10^{-5}	2.59×10^{-5}
Exit Flow	1.62×10^{-4}	1.64×10^{-4}
Concentrations (kg/m3)		
Inlet	2.1	2.1
Permeate	0.198	0.246
Exit	2.12	2.39
Pressures (kPa)		
Inlet	3447.38	3447.38
Exit	3309.48	3398.92

Table 4.5. Comparison of the forward average model with data from the ROGA-4000 spiral wound membrane available in the literature (Ohya and Taniguchi, 1975) to test the range of applicability of the amplified osmotic pressure constant of $K_\pi = 275$ kPa/kg/m3.

5.0 Results and Discussion

5.1 Model Test

Before analyzing the feed bypass system, a traditional system was tested to determine optimal performance within a range of feed flow rates and concentrations. The range of flow rates (.0001 - .0003 m^3/s) and the range of concentrations (2 - 3 kg/m^3) used for the test lie within the model's acceptable range for a brackish solution as determined in Chapter 4. The feed pressure was held constant at 3000 kPa. The test was performed using parameters for a sodium chloride solution and ROGA-4000 membranes (Table 5.1).

Figures 5.1 through 5.5 show the effect on the output of the system when feed rate and concentration are varied. At the lower feed rates, the effect of concentration polarization increased the osmotic pressure differential across the membrane which resulted in a lower permeate flow (Figure 5.1). As the feed flow increased, the turbulent mixing reduced the effects of concentration polarization which increased permeate flow. At some transition point, a maximum was reached and the negative effect of increasing hydraulic pressure loss (Figure 5.2) surpassed the positive effects of concentration polarization reduction and the permeate flow began to decrease once again. The reduction in concentration polarization that accompanied an increasing flow rate also decreased the permeate concentration (Figure 5.3).

As the inlet concentration increased, the wall concentration increased. This lead to a greater permeate concentration on the opposite side of the membrane (Figure 5.4). The increase in wall concentration also increased the osmotic pressure differential across the membrane and thus reduced the permeate flow rate (Figure 5.5).

In addition to showing the model's response to input variations, the test was used to set the inlet feed flow rate at 0.003 m^3/s for the analysis of a feed flow bypass system. This feed flow rate would allow the first membrane to approach its optimum performance as bypass around that membrane was increased.

Solution constants	Symbol	Value	Units
	K_B	2.20E-09	m/ s / kPa
	mu	1.00E-06	m2/s
	Dab	1.61E-09	m2/s
	KM	1.7	m -1/2
	pi	275	kPa/kg/m3
Membrane constants			
	Ac	3.63E-03	m2
	Dam K / t	2.3E-07	m/s
	S	0.084	m2
	X	0.014	m
	W	1.65	m
	H	2.20E-03	m
	N	50	
	L	0.7	m

Table 5.1 Parameters used in the forward averaging model for a sodium chloride solution and an ROGA-4000 membrane.

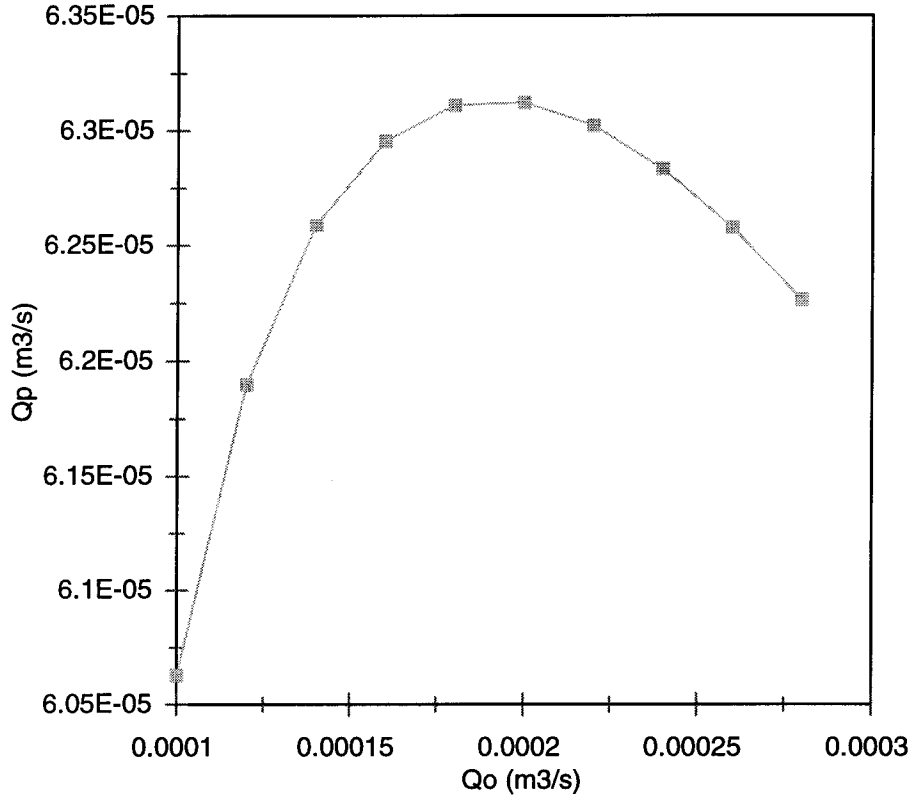

Figure 5.1 Change in permeate flow rate versus change in feed flow rate for a traditional reverse osmosis system containing three spiral wound membranes.

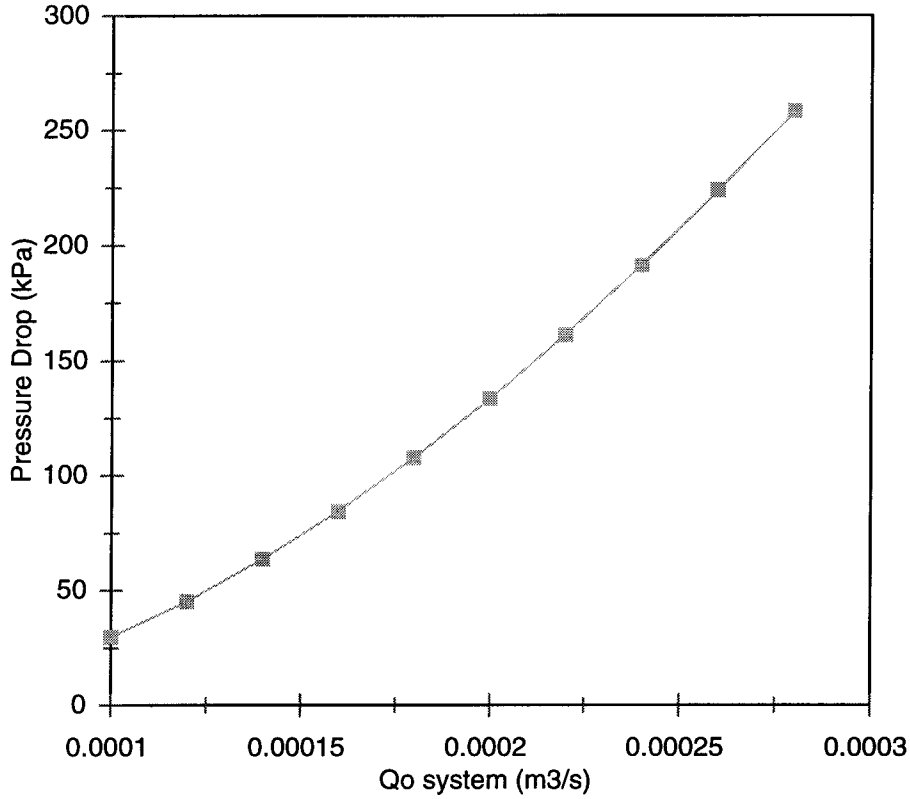

Figure 5.2 Change in axial pressure drop versus change in feed flow rate for a traditional reverse osmosis system containing three spiral wound membranes.

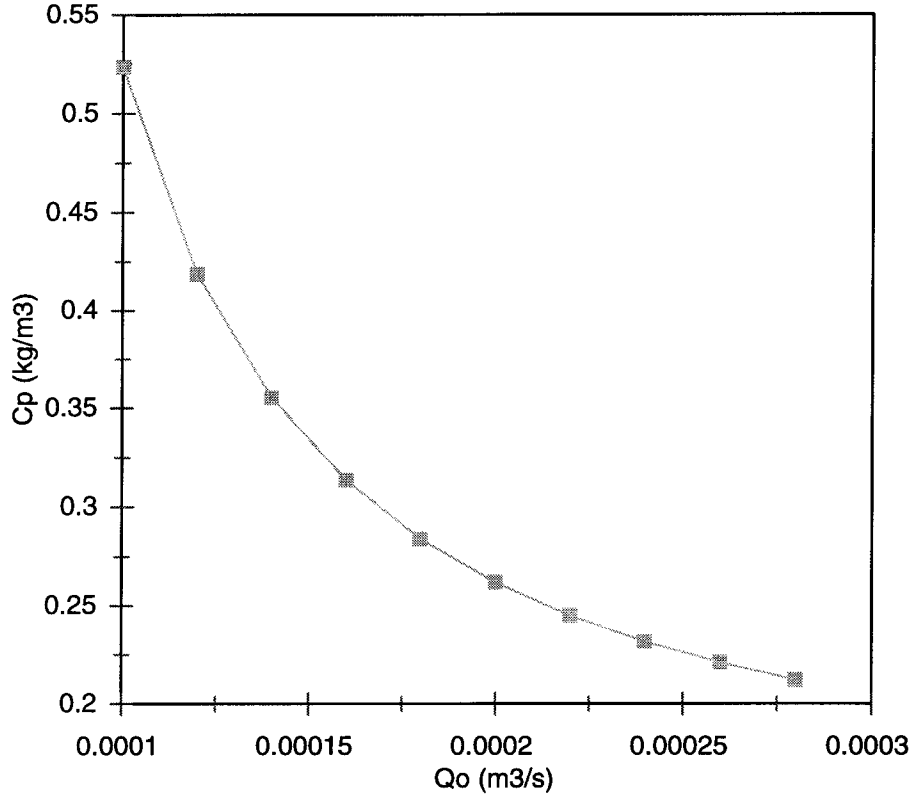

Figure 5.3 Change in permeate concentration versus change in feed flow rate for a traditional reverse osmosis system containing three spiral wound membranes.

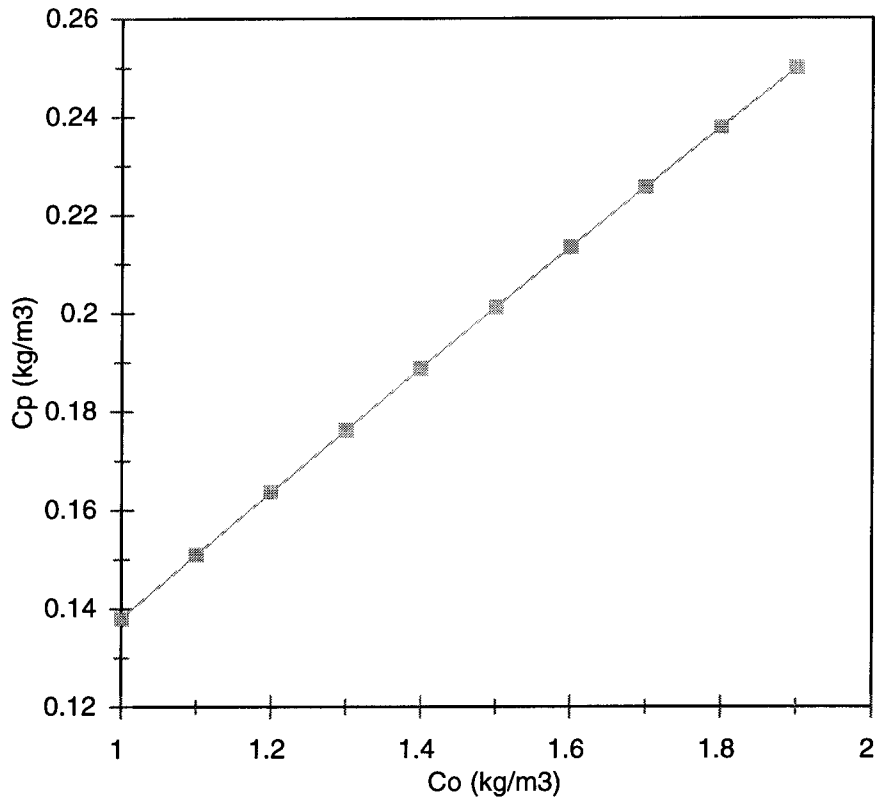

Figure 5.4 Change in permeate concentration versus change in feed concentration for a traditional reverse osmosis system containing three spiral wound membranes.

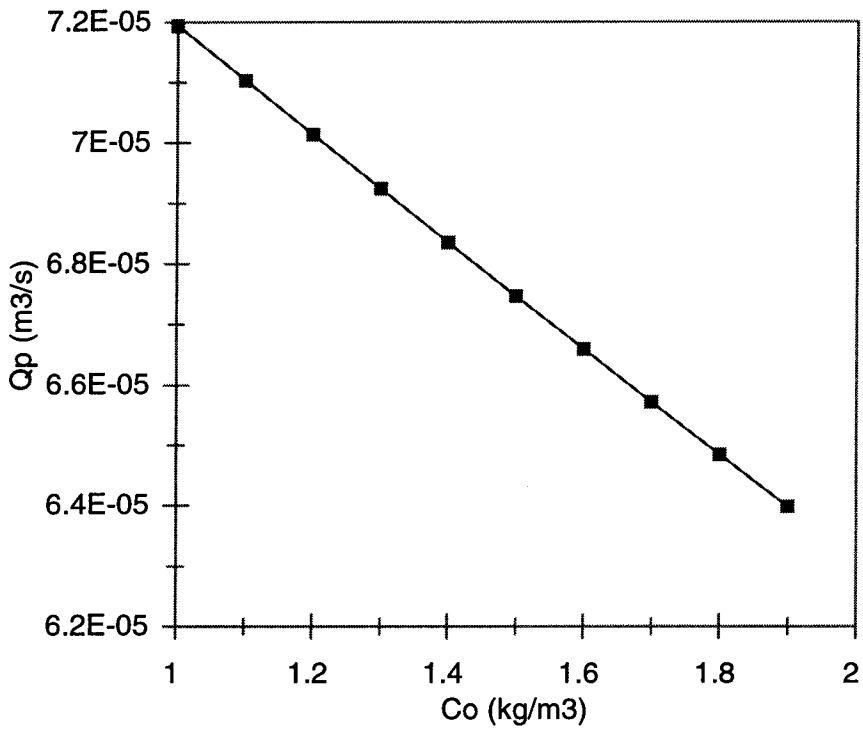

Figure 5.5 Change in permeate flow rate versus change in feed concentration for a traditional reverse osmosis system containing three spiral wound membranes.

5.2 Feed Bypass Modeled

After analyzing the performance of a traditional system, the forward averaging model was then used to simulate a feed bypass system containing three spiral wound membranes within a single pressure vessel. A percentage of the feed flow, between 0% and 40%, was allowed to bypass the first membrane and enter the second and third membranes at varying ratios. The parameters used were based on a sodium chloride solution and the ROGA-4000 membrane (Table 5.1). The inlet conditions were set at: Qo = 0.0003 m^3/s, Co = 2 kg/m^3, and Po = 3000 kPa. The effects on overall system recovery, separation and pressure loss where analyzed, the results of which can be viewed in Figure 5.6 through 5.8. Specific values taken from the figures can be read in Table 5.2.

Increasing the amount of feed flow that bypassed membrane 1 produced a slight increase in recovery from 20.63% with no bypass to 21.42% when the ratio of feed bypass entering membrane 2 to feed bypass entering membrane 3 was 30/40 in percent (Figure 5.6). The variation in bypass flow delivered to membrane 3 had a slightly greater effect on the overall system recovery than the flow entering membrane two. For example, if the bypass ratio was set at 40/0, recovery increased to 21.1%. If, on the other hand, the bypass ratio was set at 0/40, the recovery increased to a slightly higher value of 21.2%. This slight difference was due, in part, to the higher concentrations seen by membrane 3 that would inevitably be reduced by the bypass entering that membrane.

The increase in recovery was the result of a significant decrease in the amount of pressure lost through the system (Figure 5.7). With no bypass, pressure loss was almost 300 kPa; but a minium pressure loss of 125 kPa occurred at a bypass ratio of 40/40. As with recovery, the greater effects on pressure loss came with variations in the amount of flow entering membrane 3.

With such a significant decrease in the pressure drop through a bypass system, it was puzzling to witness a relatively slight increase in recovery. This initial discrepancy is explained by considering the effects of flow bypass on concentration. As seen in Figure 5.8, a decrease in feed bypass led to a decrease in separation. This decrease in separation was indicative of an increase in wall concentration which adversely affected recovery. This phenomenon, along with a more detailed analysis of the modeled feed bypass system and its effect on permeate flux, concentrations, and pressure, is discussed in following sections.

Inlet1	Bypass2	Bypass3	Pdrop	f	Y
%	%	%	kPa	%	%
100	0	0	294.75	89.77	20.63
70	10	20	207.46	88.78	21.11
70	20	10	223.82	89.03	21.06
60	20	20	192.97	88.47	21.21
30	30	40	132.55	85.29	21.42
20	40	40	125.89	82.48	21.40

Table 5.2 System response to changes in percentage of feed flow bypass diverted to membranes 2 and 3. Operating conditions are for Qo=0.0003 m^3/s, Co=2 kg/m^3, and Po= 3000 kPa. Data is taken from figures 5.6 through 5.8.

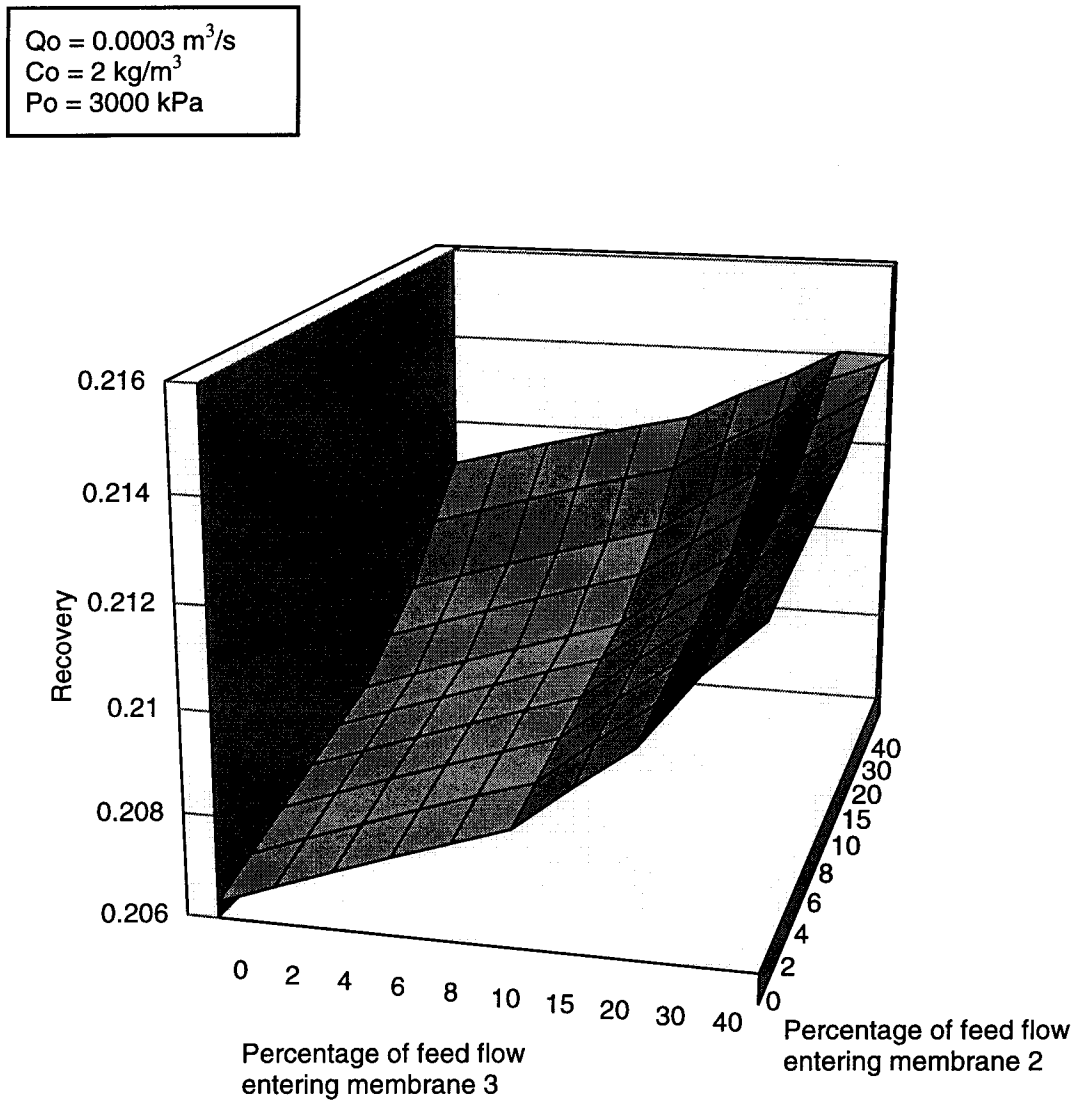

Figure 5.6 The effect of varying inlet feed bypass on overall system recovery.

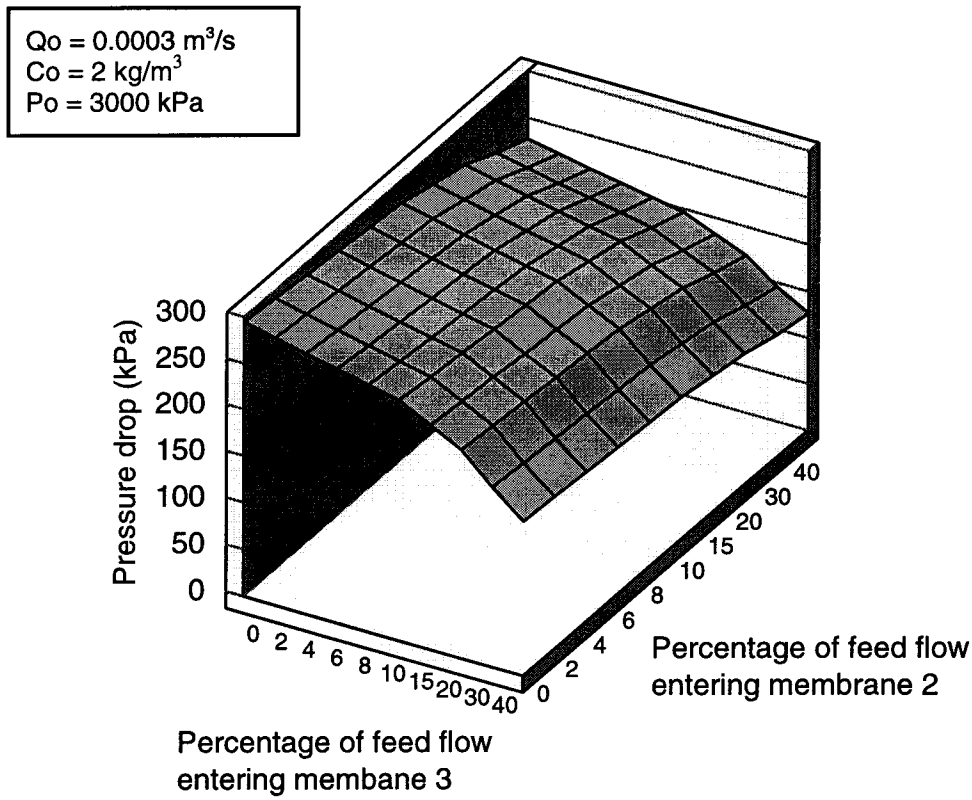

Figure 5.7 The effect of varying inlet feed bypass on overall system pressure drop.

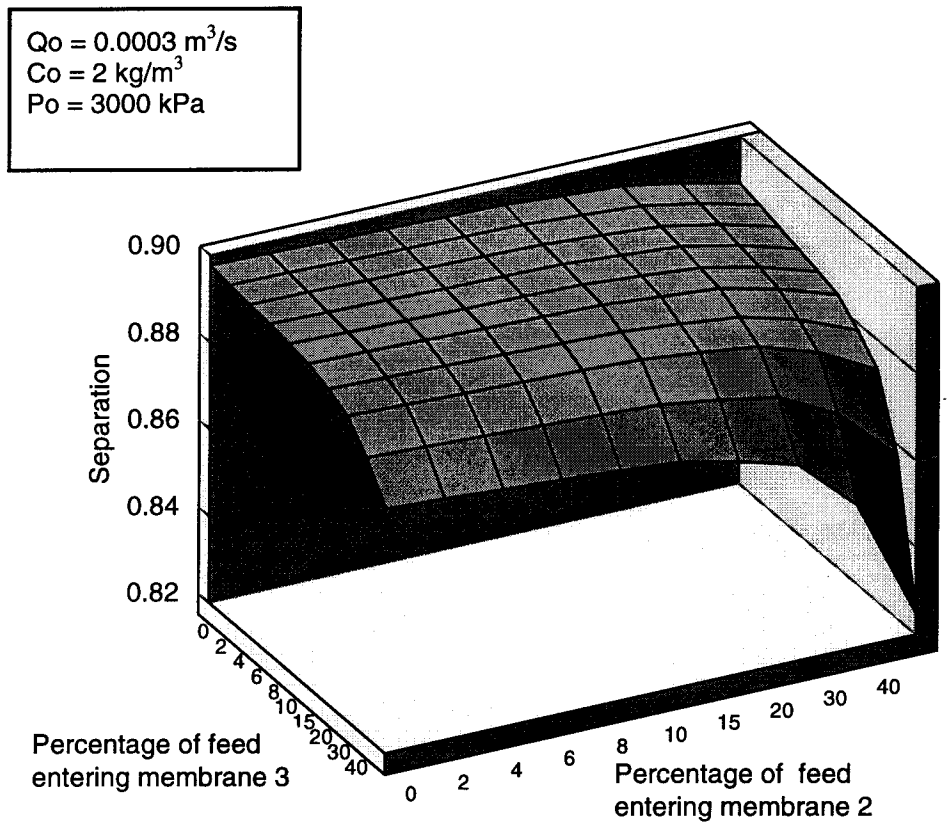

Figure 5.8 The effect of varying inlet feed bypass on overall system separation.

5.3 Detailed Analysis

The forward averaging model lent itself to a detailed analysis of the conditions within the three spiral wound membranes of the pressure vessel. With parameter conditions and inlet conditions equivalent to those in Table 5.1, a detailed analysis was performed on the system's response to:

- A change in flow rate bypassing the first membrane.
- A change in flow ratio entering the second and third membranes.

5.3.1 Analysis of Bypass Flow Rate

A bypass ratio of 0/0 was analyzed to simulate a traditional system as the control. Bypass ratios of 40/40 and 20/20 were analyzed to compare and contrast the system's response to high and low bypass flow rates. Separation and recovery for a 40/40 and 20/20 bypass system can be found in Table 5.2. The variation in flows between the bypass systems and the traditional system can clearly be seen in Figure 5.8. The spikes in flows correspond to the location of mixing between two membranes. The higher 40/40 bypass significantly reduced the flow entering the first membrane as well as the pressure drop through the first and second membranes (Figure 5.9). The pressure drop through the third membrane of both bypass systems was equivalent to the pressure drop through the third membrane of a traditional system. Because less pressure was lost through the first two membranes, the overall pressure loss was significantly less in the bypass systems.

The reduction in pressure loss resulted in greater permeate flux for the 20/20 bypass system (Figure 5.10). For the 40/40 bypass system, an increase in concentration caused the permeate flux through the first membrane to drop below that of the 20/20 bypass and the traditional system.

The adverse effects of a high feed bypass flow are clearly seen in Figure 5.11. A significant increase in bulk flow concentration occurred in the 40/40 bypass due to the reduction in cross flow velocity over the membrane surface. As the volume of water moving across the membrane surface decreased with unit time, the concentration of that water increased. This increase in bulk flow concentration led to an increase in wall concentration (Figure 5.12) which reduced the passage of solvent and increased the passage of solute (figure 5.13).

When the low bypass flow of 20/20 was compared to the higher bypass flow of 40/40, it became clear that the effects of a feed bypass, both positive and negative, were exaggerated by the higher bypass. This exaggeration made an important difference for the overall performance of the system. The lower bypass flow of 20/20 produced solvent flux values that were comparable to that of the 40/40 bypass, but the 20/20 bypass produced significantly less permeate concentrations.

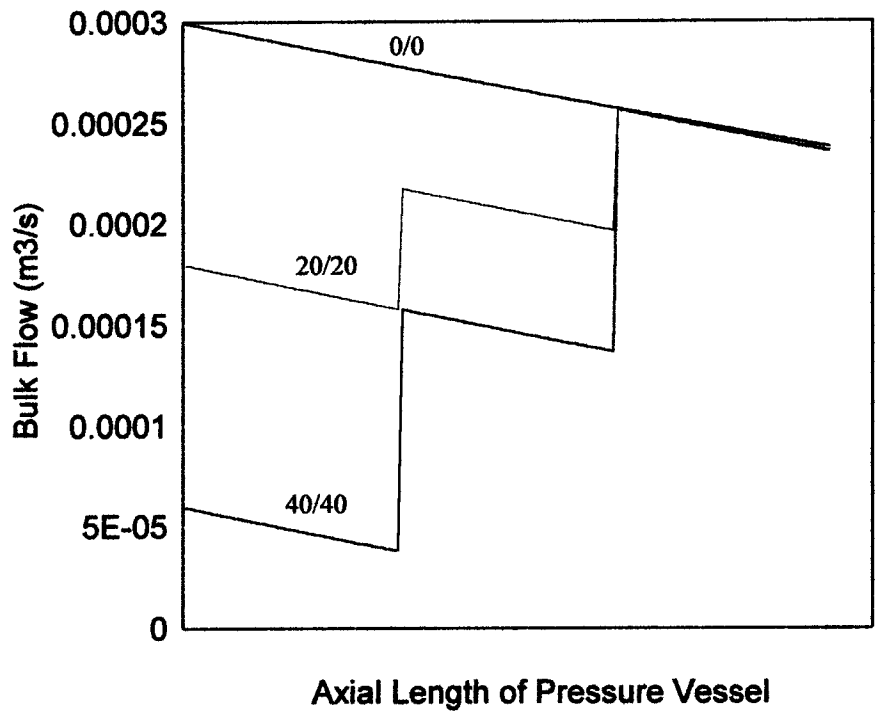

Figure 5.8 Changes in feed bypass flow rates through three membranes in series in a single pressure vessel.

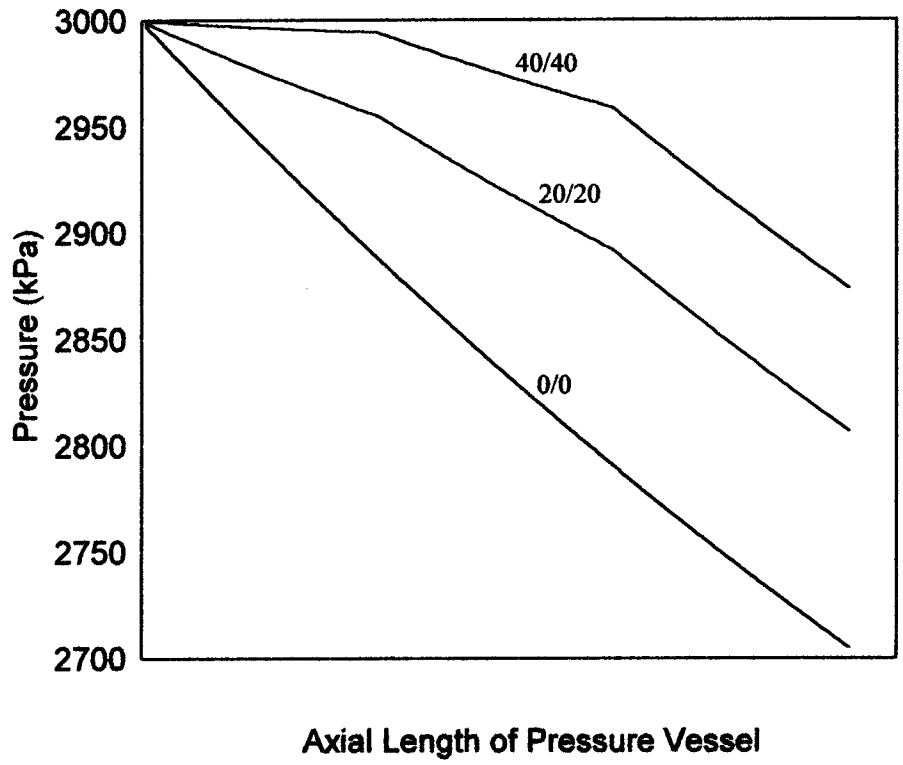

Figure 5.9 The effect of changes in bypass flow rates on pressure through three membranes in series in a single pressure vessel.

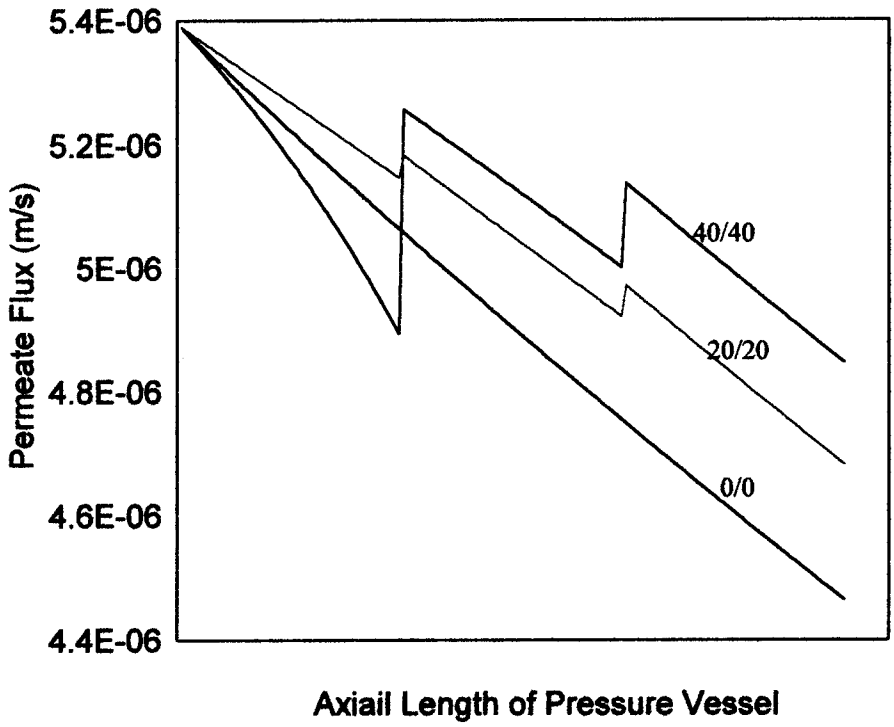

Figure 5.10 The effect of changes in bypass flow rates on permeate flux from three membranes in series in a single pressure vessel.

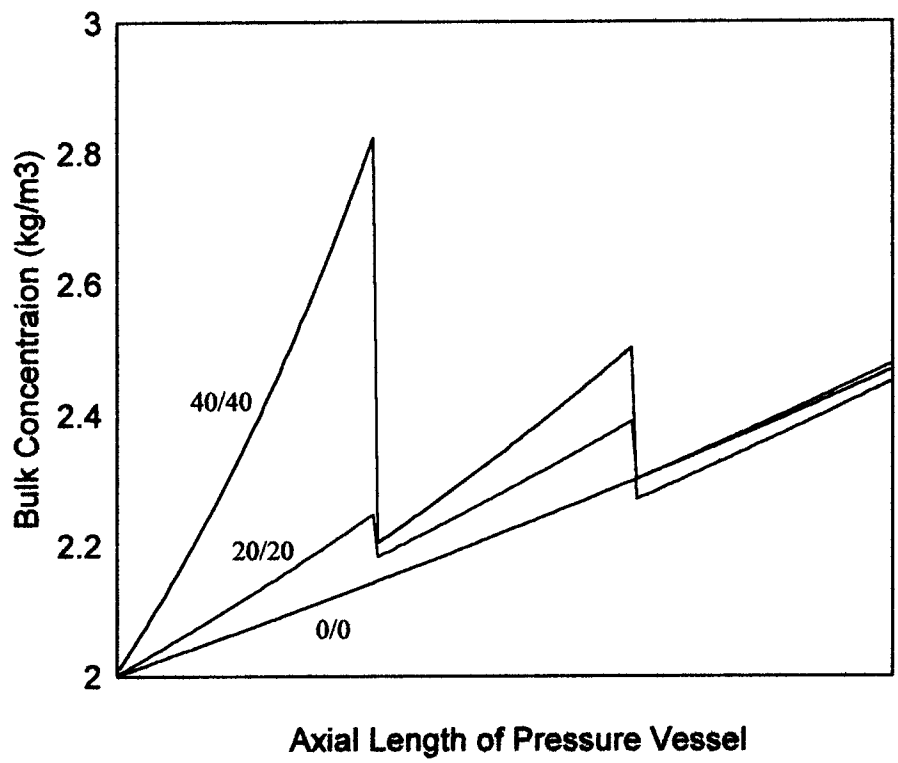

Figure 5.11 The effect of changes in bypass flow rates on the bulk concentration of three membranes in series in a single pressure vessel.

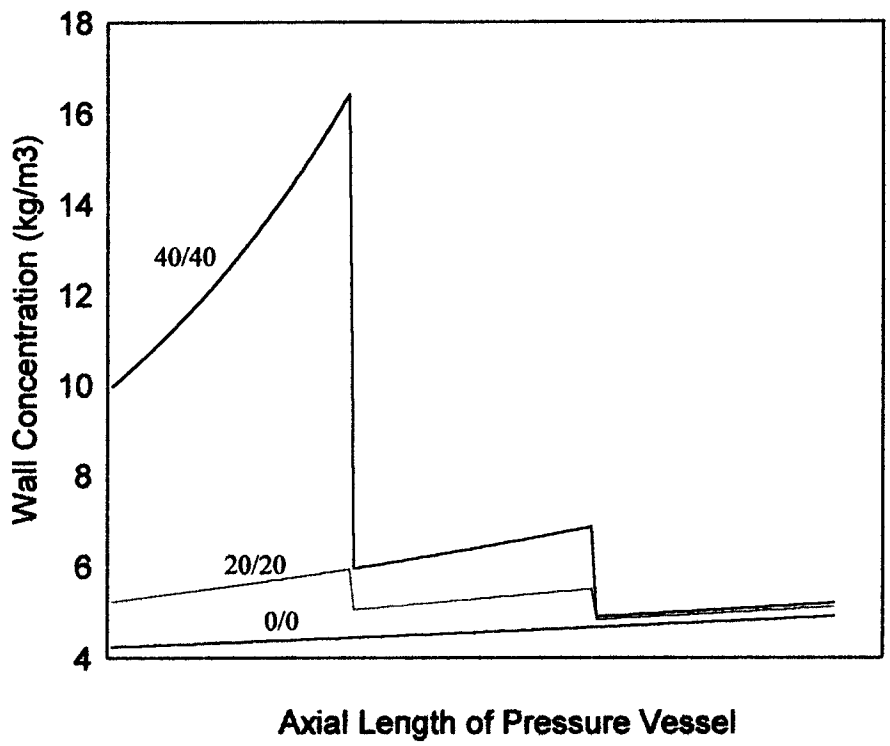

Figure 5.12 The effect of changes in bypass flow rates on the wall concentration of three membranes in series in a single pressure vessel.

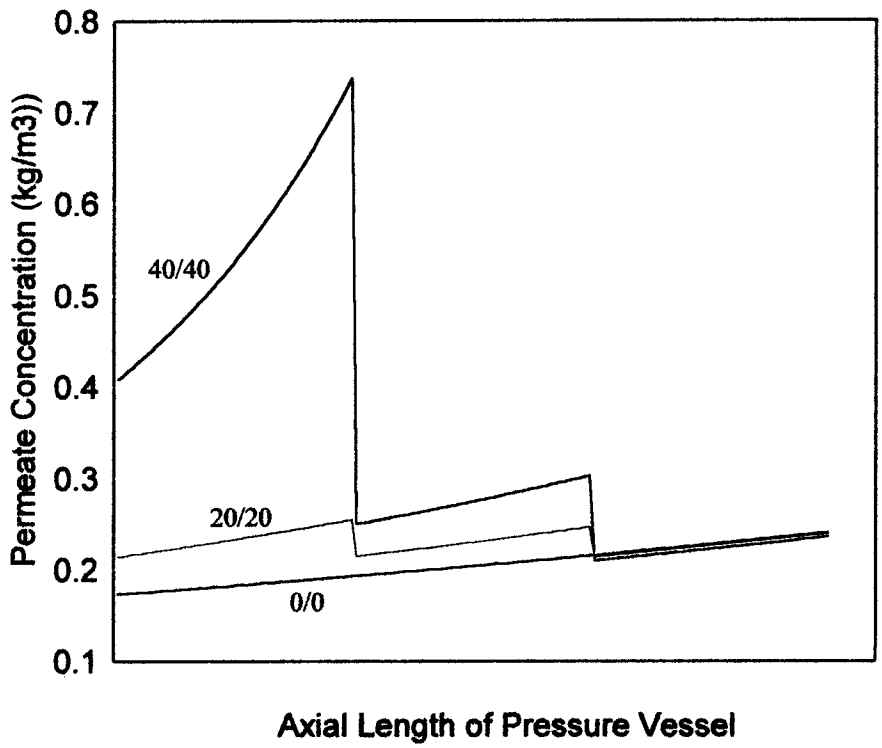

Figure 5.13 The effect of change in bypass flow rates on the permeate concentration of three membranes in series in a single pressure vessel.

5.4.2 Bypass Ratios

It was also desirable to analyze the effects of different ratios on system performance. As was mentioned in section 5.2, bypass entering the third membrane had a greater effect on system performance when compared to the bypass entering the second membrane. Two bypass flow ratios were tested. The ratio of 20/10 allowed greater bypass flow to enter the second membrane and the ratio of 10/20 allowed for greater bypass flow to enter the third membrane.

The results indicated that a bypass ratio of 20/10 would lead to slightly better system performance. Because the flow rates through the first and third membranes of the two bypass ratios were very similar, if not equivalent, the improvement was solely the result of the increased flow rate through the second membrane (Figure 5.14). The increased flow through the second membrane led to a decrease in wall concentration (Figure 5.15) and thus a decrease in permeate concentration (Figure 5.16).

With a decrease in wall concentration for the second membrane of a 20/10 bypass, one might expect the accompanying decrease in osmotic pressure to lead to an increase in permeate flux. But, as pointed out in section 5.2, the advantages of a decrease in wall concentration were offset by the increased pressure losses for a 20/10 bypass (Figure 5.17). Permeate flux was only slightly greater for a 10/20 bypass than for a 20/10 bypass (Figure 5.18).

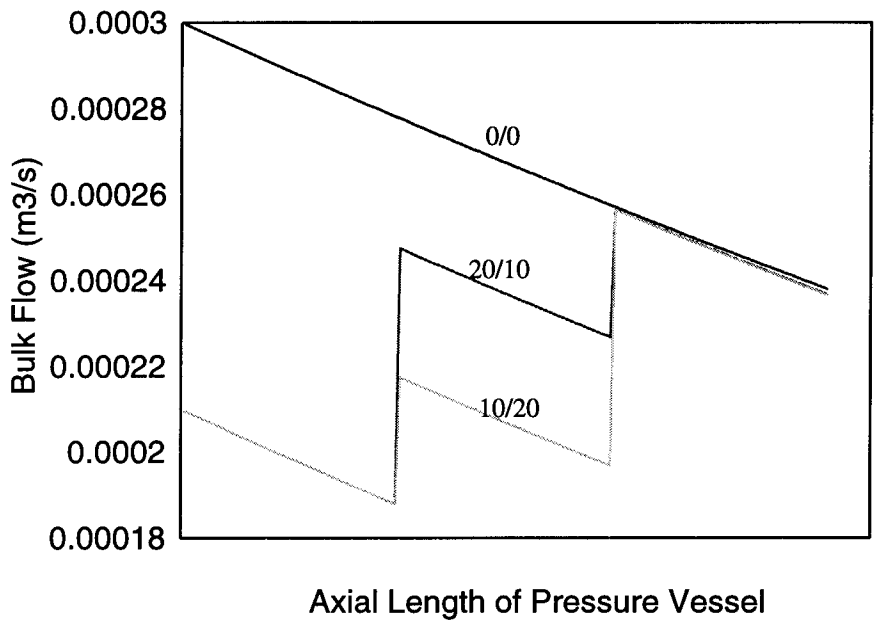

Figure 5.14 The effect of different feed bypass ratios on flow rates through three membranes in series in a single pressure vessel.

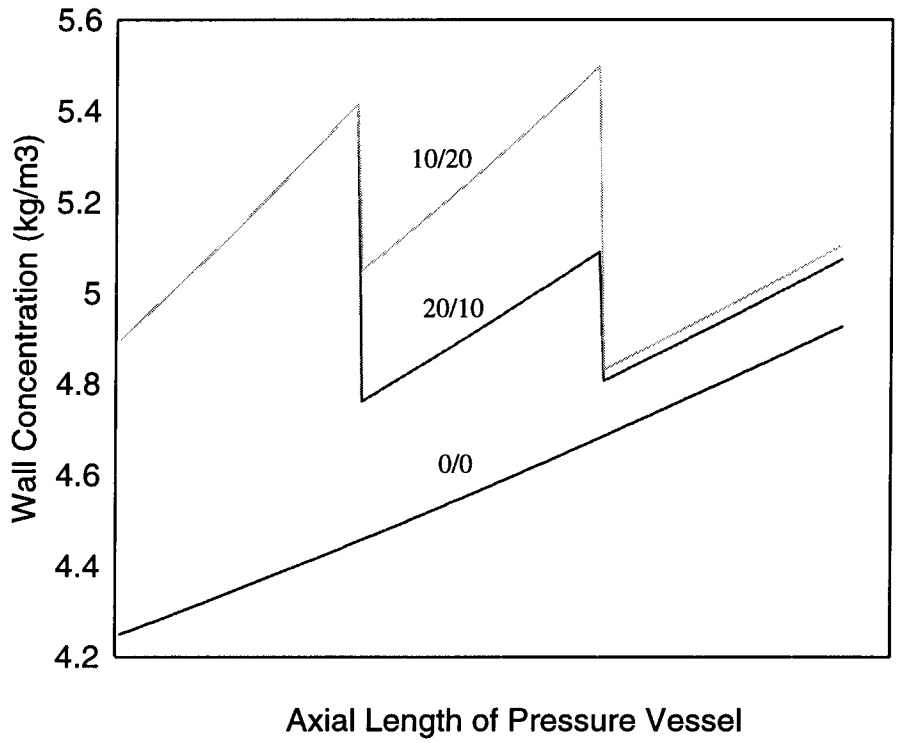

Figure 5.15 The effect of different feed bypass ratios on the wall concentration of three membranes in series in a single pressure vessel.

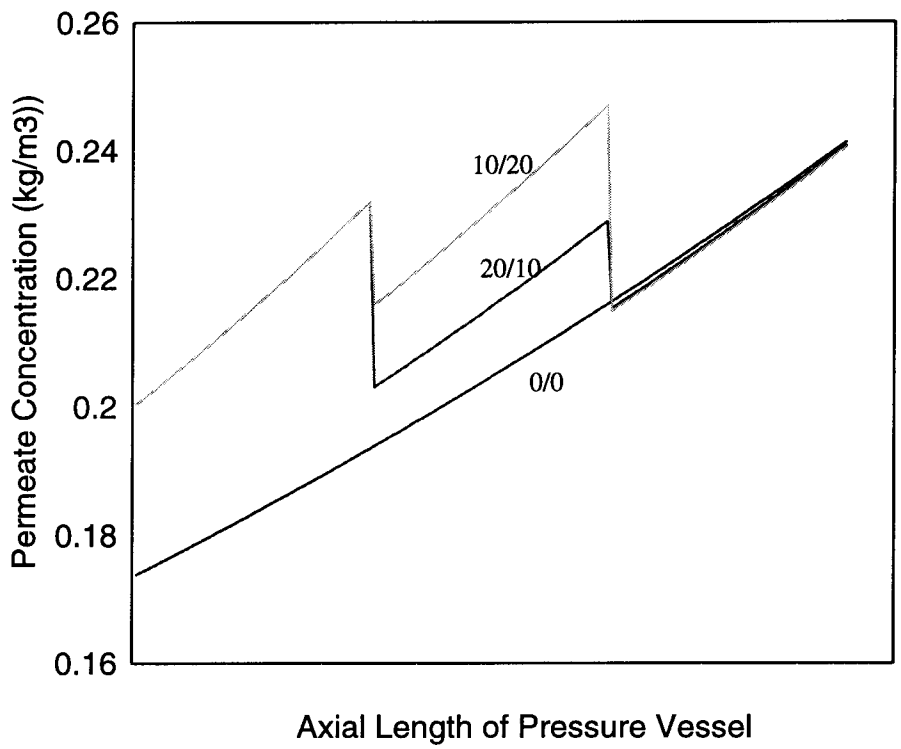

Figure 5.16 The effect of different feed bypass ratios on the permeate concentration of three membranes in series in a single pressure vessel.

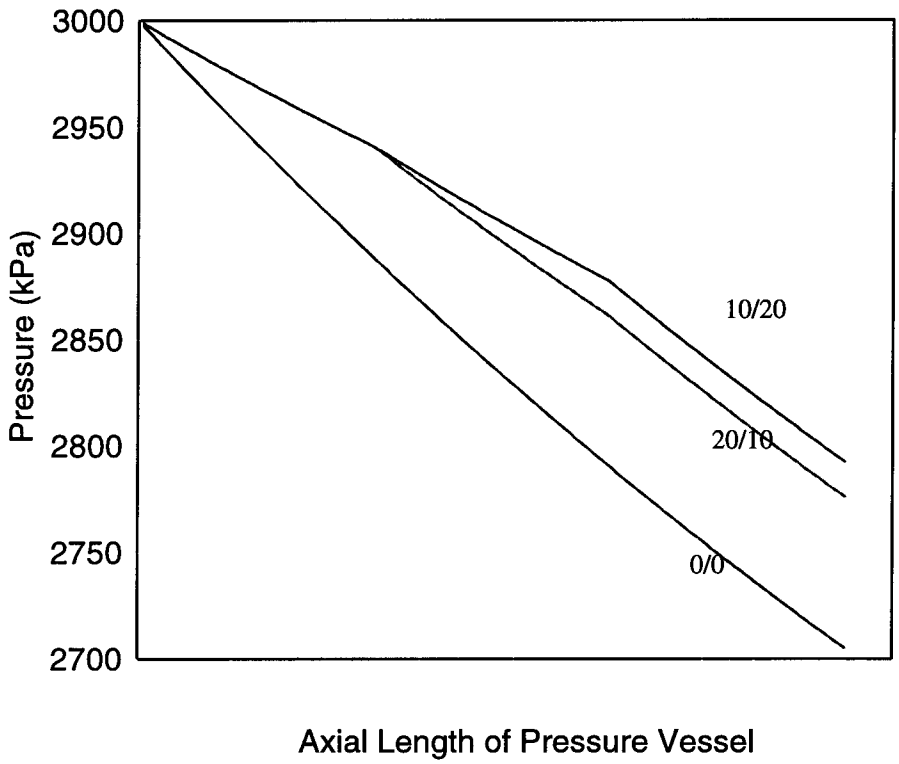

Figure 5.17 The effect of different feed bypass ratios on the pressure for three membranes in series in a single pressure vessel.

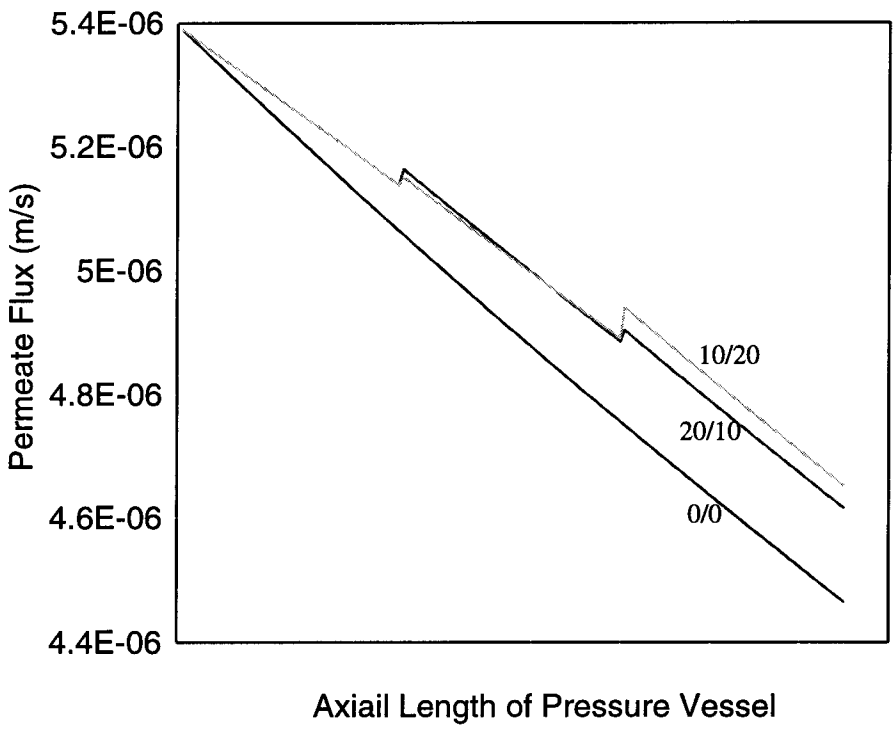

Figure 5.18 The effect of different feed bypass ratios on the permeate flux through three membranes in series in a single pressure vessel.

5.5 System Comparison

Using a bypass ratio of 20/10 and the system parameters found in Table 5.1, system performance was analyzed over a range of flowrates and concentrations as well as for variations in the membrane. The results were compared with the performance of a traditional system.

5.5.1 Flow Variations

The effect of changing flow rate on permeate concentration and pressure losses (Figures 5.19 and 5.20) was not surprising. The permeate concentration for a 20/10 bypass was slightly higher than the traditional system at all points in the range tested with the difference being slightly less at higher flow rates. Pressure losses for a 20/10 bypass were lower than those of a traditional system with the difference being slightly less at lower flow rates.

The effect of changing flow rate on permeate flow was negligible at lower flow rates. In this range, where wall concentrations became very high in both the traditional system and the feed bypass system, the permeate flow dropped off rapidly. In the higher flow range, the difference between the two systems became much greater. The feed bypass system achieved its optimum permeate flow at a higher inlet flow rate then the traditional system (Figure 5.21). This is due in part to the fact that, in the feed bypass

system, each of the three membranes approached its optimum permeate flow at similar inlet flow rates (Figure 5.22) whereas, in a traditional system, each of the three membranes achieved optimal permeate flow at slightly different inlet flow rates (Figure 5.23).

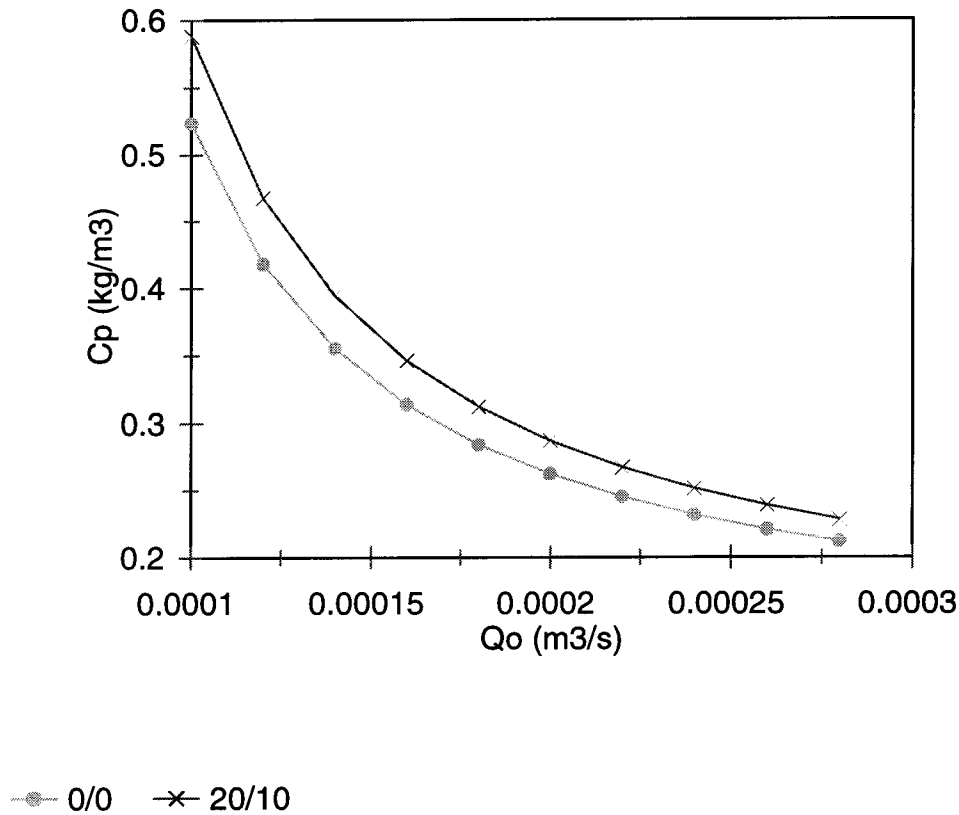

Figure 5.19 Change in permeate concentration versus change in feed flow rate for the bypass and traditional systems.

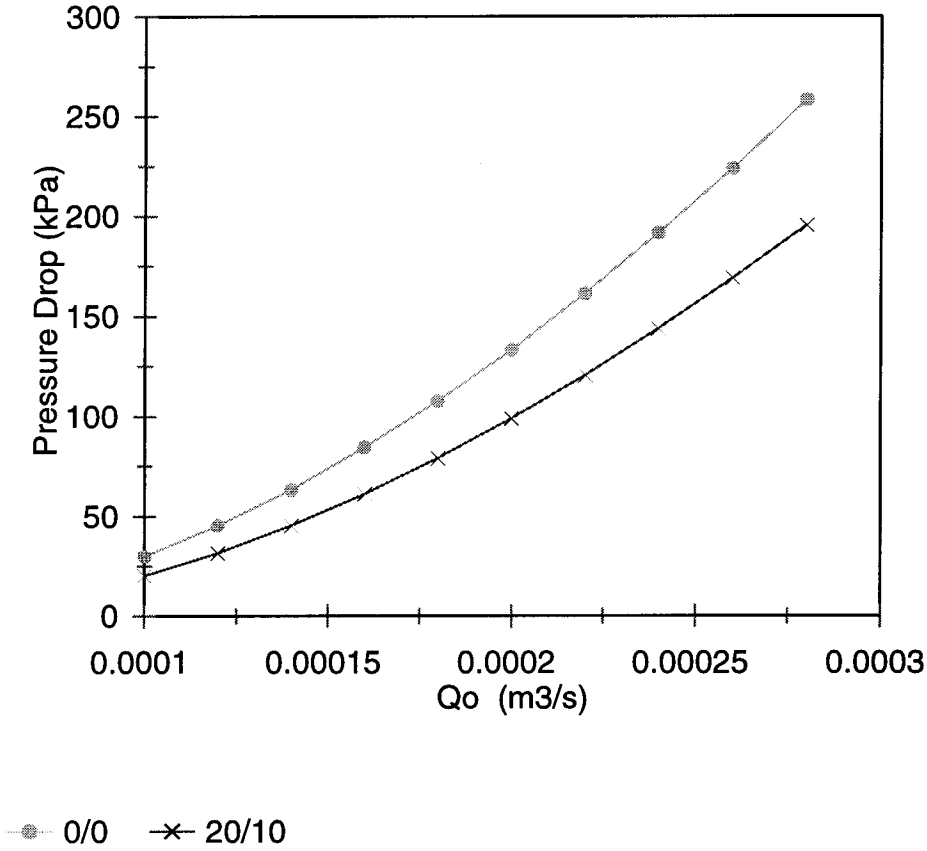

Figure 5.20 Change in axil pressure loss versus change in feed flow rate for the bypass and traditional systems.

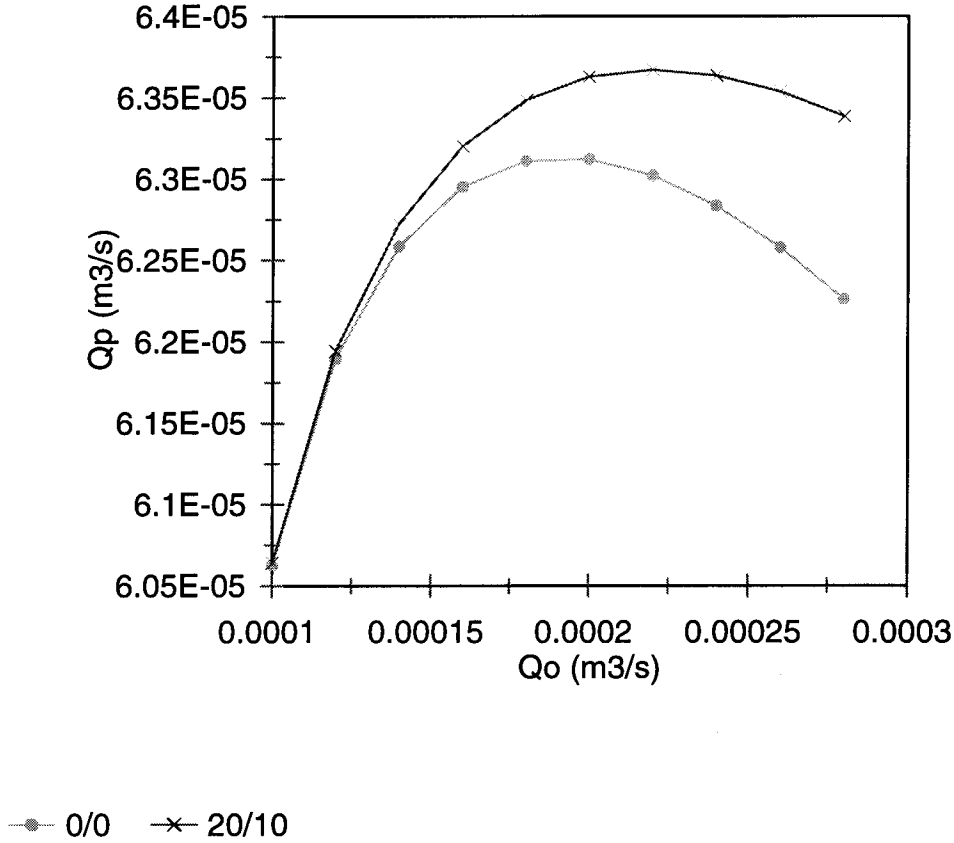

Figure 5.21 Change in permeate flow rate versus change in feed flow rate for the bypass and traditional systems.

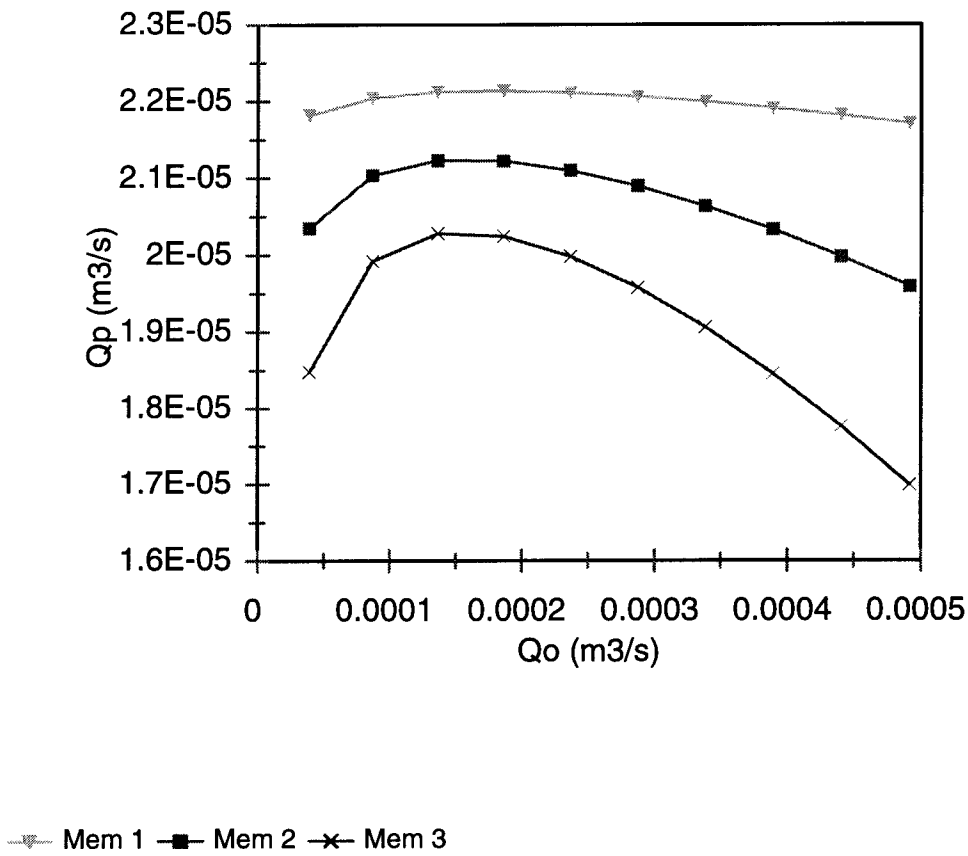

Figure 5.22 Change in permeate flow rate versus change in feed flow rate for the three membranes of a bypass system.

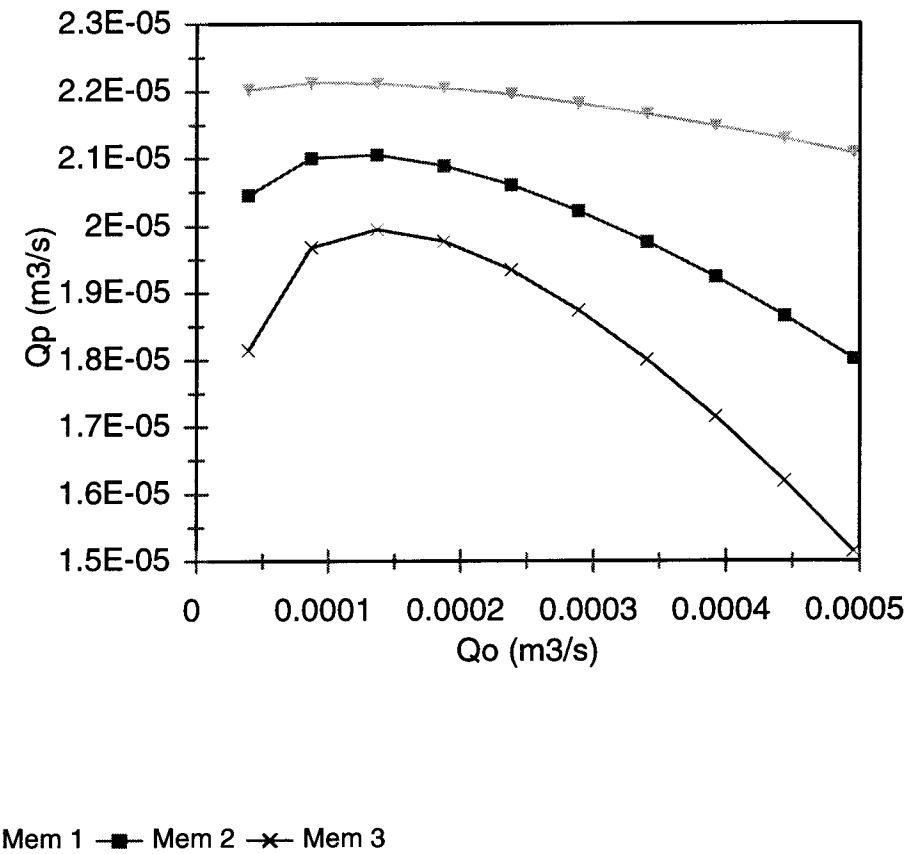

Figure 5.23 Change in permeate flow rate versus change in feed flow rate for the three membranes of a traditional system.

5.5.2 Membrane Variations

Analyzing the response of feed flow bypass to changes in the membrane size and structure was limited by the flexibility of the model. For example, changes in channel thickness returned inconclusive results because the model performs calculations based on the total cross sectional area, regardless of height and width.

Changes in flow channel width, which translate into changes in membrane size and therefore changes in cross sectional area, resulted in an increased recovery and a decrease in separation (Figure 5.24 and 5.25). The greatest changes occurred in the system with the greatest feed bypass, suggesting that the effects if a feed bypass system would be further compounded by employing larger membranes.

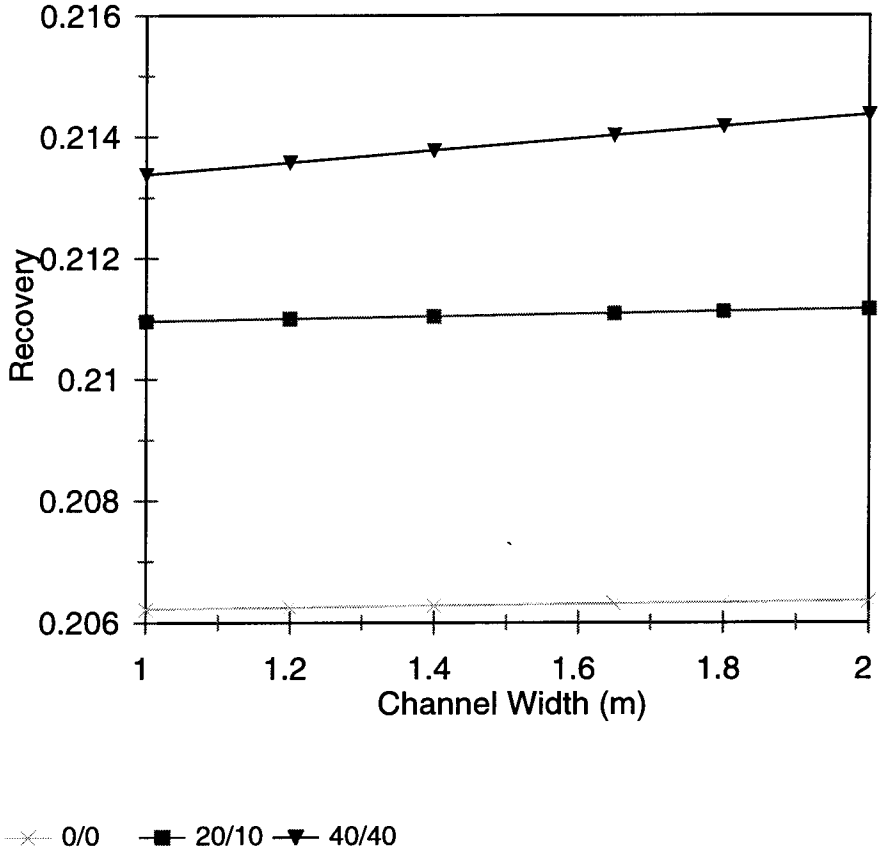

Figure 5.24 The effect of changes in membrane size on recovery for different bypass ratios.

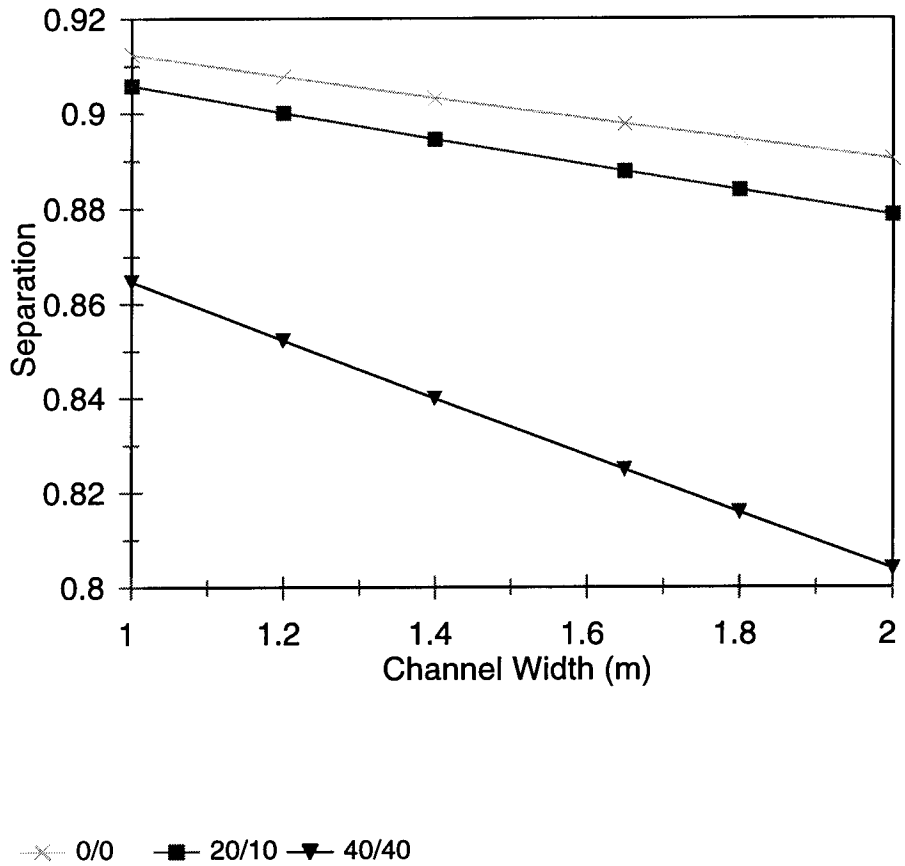

Figure 5.25 The effect of changes in membrane size on separation for different bypass ratios.

5.6 System Advantages

When considering that the diameter of the spiral wound membrane is less than the inner diameter of the pressure vessel in a feed bypass system, several advantages over the traditional system, though not related to the model, should be considered :

1. Because no dead space exists between the outer membrane surface and the inner wall of the pressure vessel, the outer membrane surface will be flushed and less fouling will occur.

2. The membranes in a feed bypass system are easier to remove and replace which would lead to a reduction in maintenance costs.

3. Because the feed bypass system does not require specially manufactured pressure vessels to maintain a seal between the membrane and the vessel wall, overall system cost could be reduced.

4. Because the bypass system allows flow to both enter and bypass the first membrane, greater flow per pressure vessel could be treated which would lead to a reduction in a plant's capital cost.

6.0 Conclusions

Reverse osmosis is a water treatment technology with the potential to address current and future water quality challenges on a large scale. Certain restrictions, including pressure loss, concentration polarization, and fouling, hinder the wider application of reverse osmosis.

This study uses a forward average model to analyze a propossed modification to the reverse osmosis process; the modification allows feed flow to bypass the first membrane in a pressure vessel and enter subsequent membranes in that same vessel. The following conclusions were made based on the modeling of a single pressure vessel containing three spiral wound membranes as well as a general consideration of the redesign:

1. Feed flow bypass offers a slight improvement in recovery, a significant reduction in pressure losses, and a decrease in separation.

2. Under the conditions analyzed, the greatest increase in recovery (21.42%) is obtained with a bypass ratio of 30/40, while the greatest separation is obtained with no bypass (a traditional system).

3. A slight increase in recovery may still be obtained, but with less of a decrease in

separation, by reducing the large buildup of concentration in membranes 1 and 2 that occurs when using a bypass ratio of 30/40. This is achieved by allowing less flow to bypass the first membrane and diverting more of that flow to membrane 2 than membrane 3.

4. The feed bypass redesign may also leads to a reduction in fouling on the outer membrane surface, easier membrane replacement, and an increase in the capacity of water treated per pressure vessel.

8.0 Appendix

Figure 8.1 Design drawing for Reverse Osmosis Feed Bypass System.(Chancellor, 1998)

9.0 References

Bhattacharyya, D. and Williams, M. (1992). *Membrane Handbook, Introduction.* Van Nostrand Reinhold, New York, NY. (edited by Winston, W. and Sirkar, K.).

Byrne, W. (1995). *Reverse Osmosis: A Practical Guide for Industrial Users.* Tall Oaks Publishing, Littleton, CO.

Carnahan, R., Graham, W. and Furukawa, D. (1999). "Effects of Flow Distribution and Electromagnetic Fields on Membrane Transport Relationships," *International Desalination Association Proceedings.* San Diego, CA.

Chancellor, D., Jensen, J. and Morin O. (1998). "A Revolutionary Gravity Assisted, Vertical Casing, RO Demonstration," *American Desalting Association.* Williamsburg, VA.

Da Costa, A., Fane, A. and Wiley, D. (1994). "Spacer Characterization and Pressure Drop Modeling in Spacer Filled Channels for Ultrafiltration." *Journal of Membrane Science,* 87, pp. 79-98.

Dickson, J.M., Spencer, J. and Costa, M.L. (1992). "Dilute Single and Mixed Solute System in a Spiral Wound Reverse Osmosis Module: Part 1: Theoretical Model

Development," *Desalination*, 89, pp. 63-88.

Gardner, T. and Engleman, R. (1997). *Sustaining Water, Easing Scarcity: A Second Update*, Population in Action International, Washington D.C.

Glater, J. (1998). "The Early History of Reverse Osmosis Membrane Development," *Desalination*, 117, pp. 297-309.

Lonsdale, H. K. (1982). "The Growth of Membrane Technology," *Journal of Membrane Science*, 10, pp. 81-181.

Madireddi, K., Badcock, R.B., Levine, B., Kim, J.H. and Stenstrom, M. K. (1999). "An Unsteady-state Model to Predict Concentration Polarization in Commercial Spiral Wound Membranes." *Journal of Membrane Science*, 157, pp. 13-34.

Matsuura, T. (1993). *Reverse Osmosis : Membrane Technology, Water Chemistry, and Industrial Applications*. Van Nostrand Reinhold, New York, NY. (Edited by Zahid Amjad).

Polyakov, V.S. and Polyakov, S.V. (1996). "On the Calculation of Reverse Osmosis Plants with Spiral Wound Membrane Elements," *Desalination,* 104, p. 215.

Porter, M.C. (1975). "Selecting the Right Membrane," *Chemical Engineering*, 71, p. 55.

Potts, D.E., Ahlert, R.C. and Wang, S. S. (1981). "A Critical Review of Fouling of Reverse Osmosis Membranes," *Desalination,* 36, pp. 235-264.

Ohya, H. and Taniguchi, Y. (1975). "An Analysis of Reveres Osmosis Characteristics of ROGA-4000 Spiral-Wound Module," *Desalination, 16*, pp. 359-373.

RO System Design with Filmtec Elements (1984). Technical Bulletin, FilmTec Corporation, Minnesota.

Scott, J. (1981). *Desalination of Seawater by Reverse Osmosis.* Noyes Data Corporation, Park Ridge, New Jersey.

Simon, P. (1998). Tapped Out, The Coming World Crisis in Water and What We Can Do About It. Welcome Rain, New York.

Sourirajan, S. (1970). *Reverse Osmosis.* Academic Press, New York, NY.

Sourirajan S. (1977). *Reverse Osmosis and Synthetic Membranes.* National Research Council Canada Publication, Ottawa, Canada.

Wessels, L.P., Van der Meer, W.G.J., Van Paassen, W.C. and Vos, G. (1998).

"Innovative Design of Nano and Ultrafiltration Plants," *Desalination,* 119, pp. 341-345.

Winograd, Y., Solan, A. and Toren, M. (1973). "Mass Transfer in Narrow Channels in the Presence of Turbulence Promoters," *Desalination,* 13, pp. 171-186.

Appendix A. Design drawing for Reverse Osmosis Feed Bypass System. (Chancellor, 1998)

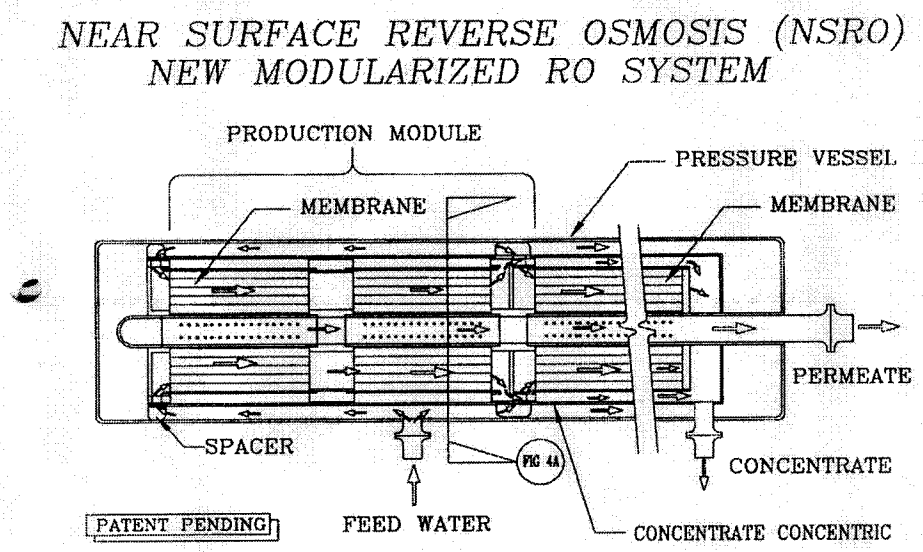

FIGURE 3